The long-term bio-geomorphic development of foredune blowouts quantified from PlanetScope imagery and Airborne LiDAR data

Name:	Eline van Inzen
Student number:	5755255
Date:	13-08-2022
e-mail:	e.l.t.vaninzen@students.uu.nl
1st supervisor:	prof. dr. Gerben Ruessink
2nd supervisor:	dr. Jana Eichel
ECTS:	45
Master:	Earth Surface Water, Utrecht University, Department of Physical Geography

Utrecht University

Frontpage image:
One blowout created in the Noordvoort project
Source: Deltares, photo Stéphanie IJff (https://www.ecoshape.org/en/concepts/enhancing-dune-dynamics/practical-applications-2/)

Abstract

Nowadays the Dutch coastal dune management is focussing more on 'dynamic preservation' of the foredunes whereby it is the objective to enhance dune biodiversity and elevate the hinterland to keep up with the sea level rise. A recent addition to this strategy is stimulating natural blowouts or digging man-made blowouts to increase the aeolian transport from the beach to the back dunes. However much is unknown about the long-term (bio)-geomorphic development of these foredune blowouts and their effectiveness on different timescales, annual and seasonal.

Here, the differences and similarities in morphological development between six different Dutch blowout sites near *Noordvoort*, *Egmond-Bergen*, *Bloemendaal*, *Schouwen* and two on *Terschelling*, are shown. A positive trend in sand area gain at the edges of the blowout with depositional lobe expansions from the end of 2016 to the beginning of 2021 is seen for *Schouwen* (40.9%, ~20169 m^2/year), *Egmond-Bergen* (36.2%, ~3473m^2/year), *Noordvoort* (27.6%,~962m^2/year), *Terschelling 2* (15.3%,~2729 m^2/year), *Bloemendaal* (15.0%,~4486 m^2/year) and *Terschelling 1* (27.5% from 2019-2021 ~8984m^2/year). Clear seasonal variations in sand area occurred around the edges of all six blowouts with peaks of the highest and lowest sand areas at the beginning of the growing season and at the end of the growing season which corresponds with the greenness cycle of vegetation. *Egmond-Bergen (*0.38x10^4 m^3/year*), Bloemendaal (*1x10^4 m^3/year) and *Terschelling 2 (*0.67x10^4 m^3/year) showed an increase in cumulative sand volume and *Noordvoort (*~1.04x10^3 and ~0.77x10^3 m^3/year*), Schouwen (*~2.2x10^4 and ~2.3x10^4 m^3/year*)* and *Terschelling 1 (*~1.75x10^4 and ~0.485x10^4 m^3/year*)* showed an increase followed by a decrease in cumulative sand volume. Sand area changes were determined since 2016 using 3x3m PlanetScope multispectral satellite imagery and volumetric changes area were determined since 2012 using LiDAR airborne elevation data.

The morphological blowout development which consisted of a deepened and widened deflation basin and a landwards expanded and migrated depositional lobe, assumed that all blowout sites were still in the geomorphological stage following the conceptual model of Schwarz et. al. (2018). Overall, no strong relation in size, age, man-made/natural or beach connection which might drive the sand area or volume increment difference, was found by looking at these results.

However this study may be the starting point for a more defined comparison between the factors that determine the obtained differences in the long-term (bio)-geomorphic blowout development. For example, distribution of the height changes for several landcover changes may determine a deposition threshold for a blowout stage transition. Furthermore, research on a considerable amount of different blowouts with detailed sand budget computation involving an increased satellite resolution and decreased time span, will be relevant.

Keywords: foredune blowouts, PlanetScope multispectral satellite imagery, LiDAR elevation data, landcover change, volumetric change, blowout development stage.

Table of contents

List of Figures

1. Introduction

Coastal dunes provide a wide range of functions and benefits for humankind (Everard et al., 2010), such as providing habitats for flora and fauna due to their unique ecosystem, facilitating drinking water, and serving as a recreational touristic attraction. And most importantly, the dunes are part of the coastal defense and protect the hinterland against marine flooding. For many decades, this last function has dominated the low-lying shore coastal dune management. These managements are focussing on erosion control and foredune stabilization by increasing the vegetation cover (Arens et al., 2013). However, this stabilization strategy is inhibiting the aeolian sand supply from the beach into the landward back dunes, resulting in two main problems; First, the existing vegetation of the back dune is no longer locally reset by sand burial. The local succession is decreasing in pioneer stages and suffers from the encroachment of late-successional tall grasses and shrubs, resulting in reduced biodiversity in general. Secondly, the reduced aeolian sand input stops the back dune from expanding in landward direction, or from growing vertically to keep up with the rising sea-level. In the future, without any change, this can endanger coastal safety for the densely populated areas below sea level.

So nowadays, the Dutch coastal management strategy is focussing on so-called 'dynamic preservation' (Arens et al., 2013), for which it is key to provide a self-maintaining ecosystem with minimal further management. A recent addition to this strategy is to reconnect the beach with the back dune by digging foredune blowouts (Ruessink et al., 2018). It is considered that this renewed beach-dune interaction, created either by artificial blowouts or by stimulating natural blowouts, provides a local harsh environment at the back dune which will enhance biodiversity and induce vertical accretion. So foredune blowouts are expected to contribute to a dynamic, resilient and biodiverse ecosystem, whereas closed or stabilized blowouts reduce these advantages.

Despite the increasing use of notches in coastal zone management, much is still unclear on blowout development over space and time at natural and managed coasts. The artificially made blowouts and stimulated natural blowouts are considered very successful for reactivating the dunes on the short term (seasons-years), but the long-term (> years) effects are not yet known. A blowout can progress through three successional blowout stages; Geomorphological stage, bio-geomorphological stage and ecological stage. These stages with their interactions and feedbacks between biotic and abiotic processes could help to understand spatial and temporal variation in blowout morphology. Therefore it is important to investigate these different blowout stages and what (bio-)geomorphic thresholds are involved. A comparative study between different blowout sites using high-resolution PlanetScope multispectral satellite imagery and LiDAR airborne elevation data might be of great value to determine the factors that influence the evolutionary blowout trends. PlanetScope data will allow investigate aerial sand and vegetation dynamics at high temporal and spatial resolution. While the LiDAR data provides insight into erosion/deposition patterns and sand budgets. Knowledge about these trends could contribute to facilitating long-lasting blowouts and dynamic preservation of a biodiverse and resilient coastal dune system.

First, the background wherein foredune dynamics, blowout initiation, development, closure, the conceptual model of the successional blowout stages and the objectives will be discussed in Chapter 2. Chapter 3 gives the background information about the six Dutch blowout site examined in the present study. The method in chapter 4 is divided into the PlanetScope and LiDAR section. Chapter 5 gives the results for each site including area and volumetric changes. The results which go in hand with the related literature will be discussed in chapter 6. Also, the improvements in the methods and options for future research are given. Chapter 7 will end this paper with the conclusion.

2. Background

2.1 Foredunes

The shore-parallel dune ridges on top of the backshore are the foredunes. These dune rows are fully developed by aeolian sand transport within vegetation. They are the most seaward dune ridge of the coast unless they are unable to form or the coast is erosional (Hesp, 2002). Foredunes are generally classified into two main types; incipient and established foredunes. Within these types of foredunes, there are still wide ecological and morphological variations.

Incipient foredunes (also called 'embryo dunes') are newly formed dunes within pioneer vegetation communities. They form due to sand accumulation and deposition within rough elements such as clumps of vegetation, individual plants, or driftwood (Hesp, 2002). These obstacles increase the aerodynamic roughness and tend to affect the wind flow by deceleration of wind velocities before vegetation, acceleration around vegetation and flow separation behind the vegetation (Nickling et al., 1990; Pye & Tsoar, 1990). This leads to aeolian deposition around for example vegetation patches (Zarnetske et al., 2015).

So vegetation specifications are an important factor in the morphological development and growth rate of the embryo dune (Hesp, 2002). *Ammophila*, which is the most dominant at the European foredunes, is a tall and dense vegetation species that decreases the wind velocities causing hummocky peaked dune types. While lower less dense rhizomatous species, such as *Spinifex* or *Ipomoea* lead to less hummocky, low dune forms (Davies, 1980; Hesp, 1989). Seasonal variations determine the vegetation distribution and density causing seasonal differences in growth rates and sand transport patterns (Hesp, 2002). The vegetation species and therefore the density, morphology, distribution and height together with aeolian sand supply rates determine the morphological variation of the foredunes (Hesp, 1989; Musick et al., 1996; Wilson et al., 1998; Zarnetske et al., 2015). Also, this determines if the embryo dune will erode or will develop further into an established foredune.

Established foredunes are the result of a successful incipient foredunes development. The size, volume and morphological complexity of established foredunes differ. Also, the vegetation type has mostly changed to more woody persistent stages. The morphological development of established foredunes depends on several factors; Sand supply, vegetation cover, vegetation species, aeolian sand accretion or erosion rates, frequency and magnitude of wind and wave forces, occurrence and magnitude of storm erosions, dune scraping and overwash, beach or barrier state, seawater level and human impact (Hesp, 2002).

The beach width, sand supply and wind regime are the main controlling factors if all the other factors are equal (Davidson-Arnott & Law, 1996). Small foredunes occur on reflective beaches which are narrow and have a minimal potential sediment supply, while large foredunes occur on high energetic dissipative beaches which are wide and have the maximum potential sediment supply (Sherman & Lyons, 1994). These large foredune complexes are rare and occur mostly on erosional coasts where humans control the foredune height artificially by nourishment and maintaining the absolute lee slope stability. This is the case in large parts of the Dutch coast.

Hesp (2002) made a five-step classification (Figure 1) in how the foredune evolves using previous classification methods. Foredunes mostly remain in a particular morpho-ecological stage but also may progress through an (reversed) evolutionary sequence (erosion or accretion cycle) under certain climate conditions. Stage 1 represents a stable densely vegetated foredune and the final stage 5 is a

severely eroded foredune complex. A foredune may progress through the stages 1 to 5 in an erosional cycle as aeolian erosion, wave erosion and a decline in vegetation cover take place. The erosional sequence may be reversed as rehabilitation of vegetation, stabilization and reduced wave and aeolian erosion take place. Then the foredune may progress through stages the 5 to 3 in the accretion cycle. It is unlikely that a foredune in stage 5 will revert to stage 1 or 2, because not all the erosional hollows and lower areas will be filled up with sand accretion. However a stage 5 foredune complex might continue to erode and initiate a new incipient foredune seaward which finally becomes a stage 1 foredune.

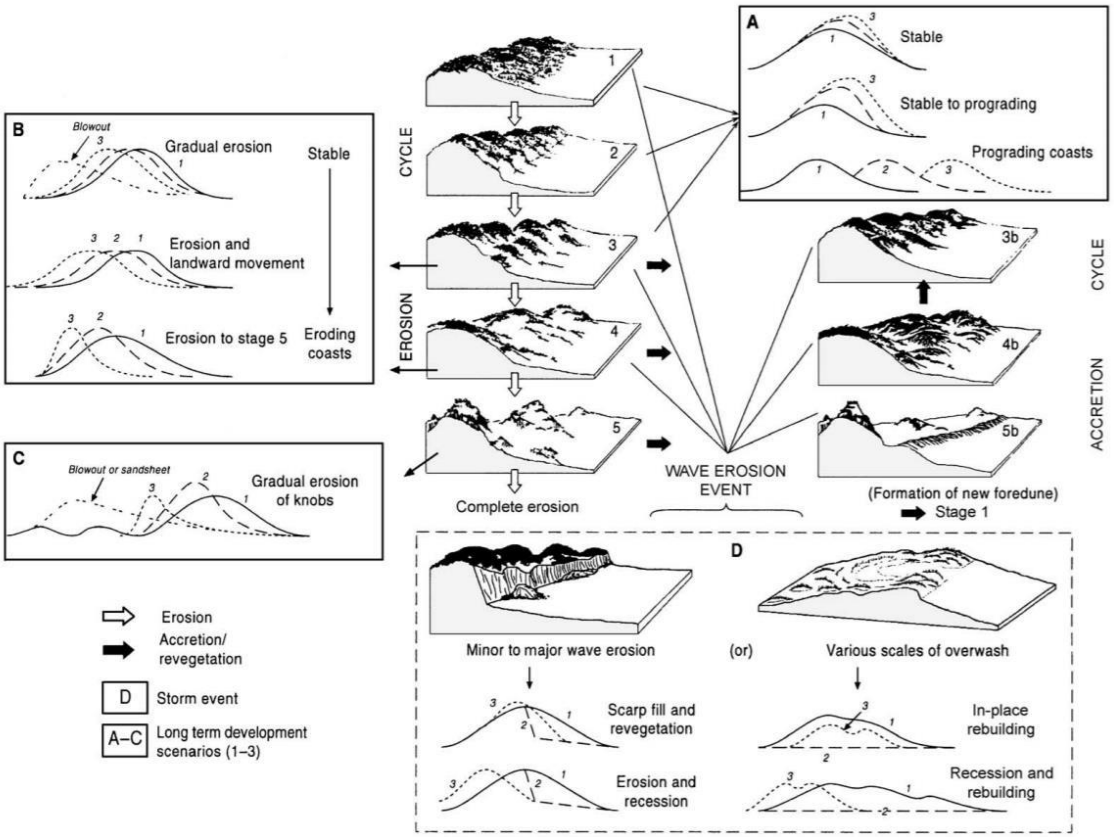

Figure 1 Model of established foredune morphology evolution with morpho-ecological stages (Types 1 to 5)(Hesp P, 2002).

2.2 Blowouts

Blowouts are defined as depressions in a sand deposition. Sand accumulates on its adjacent depositional lobe. The sandy erosional landform is a saucer,- cup- or trough-shape, resulting in the classification of two primary types, namely saucer and trough blowouts (Cooper, 1958). The saucer blowouts often occur as shallow dishes with a semi-circular shape, while trough blowouts have deep deflations basins with steep erosional walls and are generally more elongated. These blowout complexes consist of a depositional lobe, deflation basin and erosional walls (Figure 2) (Hesp, 2002). In this research the whole blowout complex is often referred as 'blowout' with its three morphological features. In the case when a notch is excavated in the foredune this this will also be referred as a deflation basin of a (artificially) blowout.

There is a large temporal and spatial variability in blowout morphologies in nature. Several factors determine the initial shape, size and location of the blowout (Hesp, 2002). This development depends on the processes disturbing the dune surface and therefore indirectly the initial depression, for example, the current dune morphology, vegetation cover, vegetation species, wind magnitude and wind direction(Davies, 1980; Gares & Nordstrom, 1987).

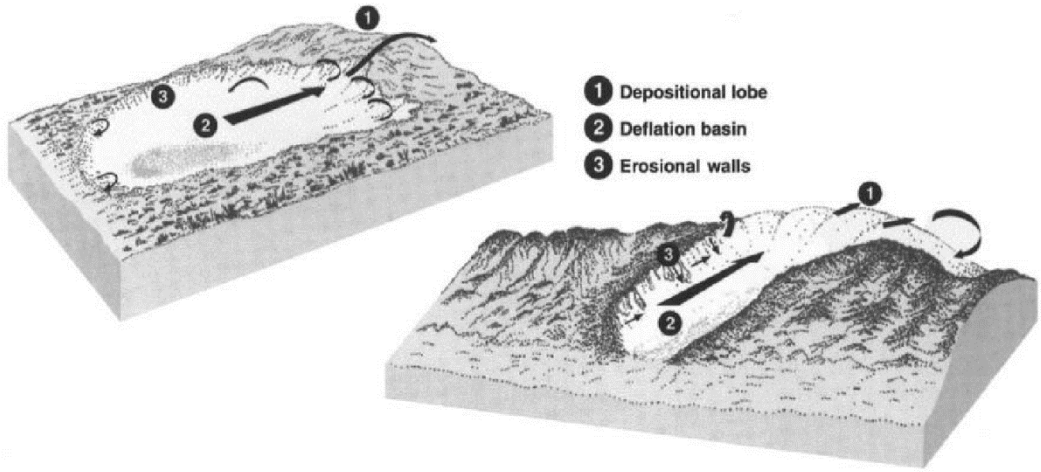

Figure 2 Schematic diagrams of a saucer and a trough blowout with their morphological units and wind flow patterns (Hesp, 2002)

2.2.1 Initiation

The initiation of blowouts occurs particularly on coastal dune environments with eroding and/or receding beaches and foredunes but also in accretionary, stable environments. The specific location in the foredune is determined by geomorphologic or vegetation-induced discontinuities. Hesp (2002) mentioned seven ways in how these discontinuities are formed and how the blowout will be initiated;

(1) Wave erosion along the seaward face of the dune which causes sufficiently narrowing of the dune. In combination with wind erosion, the poorly vegetated and lower weaker parts of the foredune starts to erode and slump. Geomorphological discontinuities in the foredune can form as a result of alongshore differences in dune erosion after a storm (de Winter et al., 2015; Splinter et al., 2018) The geomorphological discontinuities in the wind flow over the foredune crest result the formation of a potential blowout (Garès & Pease, 2015).

(2) The topography determined by the initial dune morphology, causes an accelerated and funnelled airflow over small scarps or cliffs in the dune. This results in higher erosional rates which increases the depression and onsets a blowout. The processes are the same as described in the previous initiation way (1).

(3) Climate changes in the past have contributed to blowout initiation and are expected to be so in the future (Pye et al., 2014). A weak vegetation cover due to a long-lasting dry and arid period with strong winds followed by short heavy rainfall influences the blowout development. Also prolonged changes in wind velocity and direction were drivers for the onset.

(4) The spatial and temporal variation in vegetation cover, species and density alongshore contribute to blowout initiation. Areas of less vegetation cover due to for example soil nutrient depletion, localized aridity or animal grazing enhances erosion. This is because the vegetation induced discontinuities cause a local increase in bed shear stress and the possibility for underlying sand to erode (Schwarz et al., 2018). This will finally initiate a blowout.

(5) Water erosion may contribute to blowout initiation but is not widely recognized. Intense rainfall causes surface erosion which may form rills and gullies. The wind may be accelerated within these gullies resulting in blowout initiation.

(6) Very high rates of wind erosion caused by storms and hurricanes will undermine, erode and bury vegetation. This results in bare areas of sand wherein blowouts can form.

(7) The human impact on the coastal dunes may initiate blowouts. Due to weakening or removal of vegetation by trail formation or due to implementation of coastal management strategies (Arens et al., 2004).

2.2.2 Development

The blowout morphology is defined throughout its development whereby sand from the deflation basin and the erosional walls is transported by the wind and deposited on the depositional lobe or further in the back dunes. Hereby the shape of the blowout evolves by the deepening of the deflation basin, the erosion of the walls and the expansion of the depositional lobe. For the development of the trough and saucer blowout, distinct processes are the driver.

Trough blowout

In a trough blowout, the wind direction is the dominating factor of sand transport. The distinct blowout topography causes steering and acceleration of the wind resulting in a jet flow. The wind direction is the dependent factor in the formation of the jet flow. The dominating wind direction is often onshore (Bate & Ferguson, 1996), but also oblique winds up to 50 degrees can be redirected into the trough (Hesp & Hyde, 1996; Huggett, 2007). In this case, it may double the sand transport rates in the blowout relative to the beach (Hesp & Hyde, 1996), resulting in a positive feedback between the wind field and the topographical evolution which enhances the erosional rates at the deflation basin. The deflation basin erosion causes widening and deepening of the trough blowout. The deepening is limited to the deflation basin base level which is often related to the groundwater table or an immobile layer (Barchyn & Hugenholtz, 2013a). The widening happens through undercutting and slumping of the erosional side walls whereby the collapsed material is transported downwind and deposited on the depositional lobe (Hesp & Hyde, 1996; Ruessink et al., 2018). Also at the edges of the blowout deposition of sand occur because the wind flow is separated and decelerated at the crests of the depositional lobe and the side walls. This results in the expansion of the depositional lobes landwards (Huggett, 2007) and the formation of rim dunes, making the trough blowout morphology even more pronounced.

Saucer blowout

For a saucer blowout, the development is mainly driven by the availability of sand supply (Schwarz et al., 2018). This is because both wind acceleration (Pluis & van Boxel, 1993) and wind deceleration (Smyth et al., 2012) are observed in the deflation basin. In a saucer blowout, erosion takes place at the deflation basin and at the windward blowout edge while deposition takes place at the downwind edge, generating a depositional lobe. (Miyanishi & Johnson, 2007). The feedback even becomes negative resulting in a reduced wind acceleration or wind deceleration in the blowout mouth. Deposition of sand occurs in the deflation basin and in time the blowout will close (Schwarz et al., 2018).

The morphological evolution of the blowout impacts on the vegetation. The stability of the blowout sediment bed is the dominant factor for plant survival (Maun, 2009; Miyanishi & Johnson, 2007). Schwarz et. al (2018) defined two blowout morphology processes controlling the vegetation survival; the dominating erosion at the deflation basin and the dominating accretion on the depositional lobe. The vulnerability of plants to erosion and deposition depends on the plant species, blowout development stage and the growing season (M. A. Maun, 1998).

Erosion in the deflation basin

Each plant development state (seeds, seedlings, or developed plants) reacts differently to erosion. Periodic erosion may be beneficial for seed establishment when the burying depth reaches 2-7 centimetres (Cheplick & Grandstaff, 1997). The re-colonization of these seed banks will only happen in relatively young deposits since buried seeds remain viable for up to 5-20 years (Maun, 1998). Continuous erosion will lead to seed bank depletion and the existing seedlings will not survive due to dehydration of their root system (Maun, 2009; Maun, 1994). Nevertheless erosion of the deflation

basin also brings the sediment closer to the groundwater table increasing the soil moisture. This results in less further erosion and therefore the possibility for vegetation colonization. Developed plants stabilize the side walls of the blowout. Erosion of the deflation basin results in oversteepening and finally collapsing of the side walls whereby vegetation blocks ended up in the deflation basin (Hesp & Walker, 2012).

Accretion on the depositional lobe

Maun (1998) classified seedlings and developed plants based on their resistance to sand burial; burial-intolerant (I), burial-tolerant (II), and burial-dependent (III) (Figure 3). Burial-intolerant species decrease in condition after increasing sand accretion, burial-tolerant species are not affected until a specific threshold is reached and burial-dependent species increase in condition until a specific threshold is reached. The plant condition is not always affected whenever vital parts for photosynthesis are still aboveground. Most stressful is the decrease in available oxygen (M. Maun, 2009) and therefore plants must survive periods of low oxygen before roots can develop further. However complete burial, with all three species, leads to plant death as seen in Figure 3.

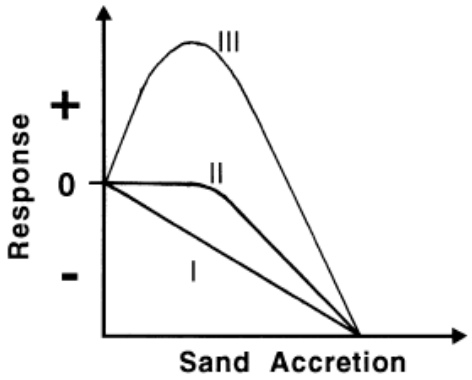

Figure 3 Plant response to sand accretion for three different vegetation species. (I) Burial-intolerant (II) Burial-tolerant (III) Burial-dependent vegetation (Maun M.A. 1998, adapted by Schwarz et al., 2018).

So when a critical blowout shape is reached, the wind flow on the deflation basin will not accelerate anymore but will reduce (Hugenholtz & Wolfe, 2006). This may lead to less sand accretion on the depositional lobe and therefore enhanced circumstances for vegetation establishment. Whereby the coupled plant growth is depending on its plant stress response. In other words, the balance between accretion or erosion and the vegetation tolerance for accretion or erosion (Barchyn & Hugenholtz, 2012).

2.2.3 Closure

Blowout closure or in other words, stabilization of the blowout, happens when the critical blowout size has reached. Then the morphology of the blowout is not capable of transporting sand through the deflation basin anymore. The blowout is stabilized by the growth of vegetation resulting in the formation of incipient foredunes across the throat of the blowout. The development of the incipient foredune prevents further erosion of the deflation basin or the erosional side-walls and defines the blowout closure (Schwarz et al., 2018). The wind threshold needed for the blowout initiation is higher than the wind energy threshold for vegetation re-establishment which is related to the vegetation's altered physical sediment structure (Feagin et al., 2015). So biogenic or human disturbances, such as extreme winds, fires and aridity changes, can drive the blowout reactivation or maintenance (Barchyn & Hugenholtz, 2013).

The vegetation plays an important role in the blowout stabilization and therefore its closure since it can influence the morphology. Germinating seeds, rhizomes fragments from the rim mass slumping or lateral rhizome growth from the side walls induce the vegetation re-colonization (Lee, 1995). The broken rhizomes and clonal rhizomes are less vulnerable to wind and grow faster than the seedlings (Maun, 2009). Therefore they are capable of recolonizing the most disturbing area of a blowout, the deflation basin. The depositional lobes are less disturbed by the wind and provide a better environment for seedlings to germinate. Also temporal variation determines the seedling germination. In temperate systems, herbaceous plants like *Ammophila* are fully developed in summer and disperse seeds in autumn, leading to seedling emergence in late spring (M. Maun, 2009). Moreover, the seeds need a disturbance-free period to increase their survival against stress sufficiently enough (Balke et al., 2014). This concept of the window of opportunity linked to climate conditions can shape the development of the blowout.

So the vegetation re-colonization depends on the interaction between the environmental factors and the different plant species. Therefore the plant growth and blowout stabilization are driven by the three main factors: The availability of the sediment originating outside the blowout, vegetation type and climate condition variability (Schwarz et al., 2018).

2.2.4 Conceptual model: Three successional stages

As described above, the evolution of a blowout depends on biotic and abiotic processes. Feedbacks between those processes determine the evolution of a blowout which can be divided into three successional stages; Geomorphological stage, bio-geomorphological stage and ecological stage (Corenblit et al., 2015; Schwarz et al., 2018). Figure 4 shows the stages with the physical disturbance intensity, the intensity of biological interactions and the strength of biogeomorphologic interactions based on the concept of Corenblit et al., (2015).

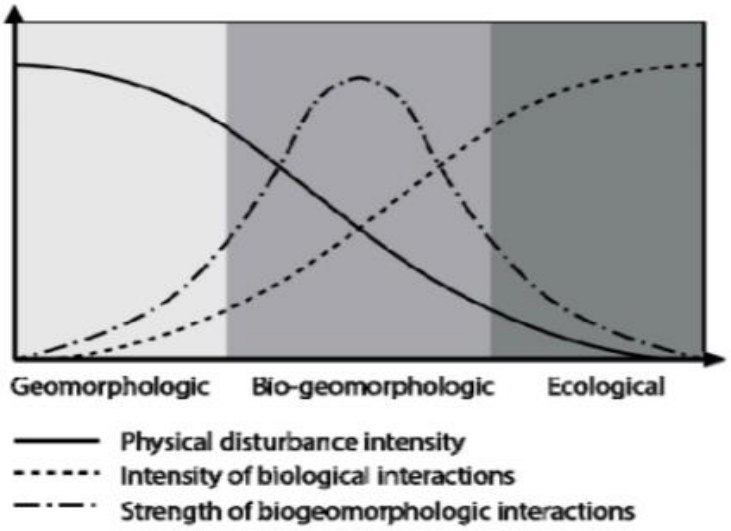

Figure 4 Three stages; Geomorphologic, bio-geomorphologic and ecological with the physical disturbance intensity, the intensity of biological interactions and the strength of biogeomorphologic interactions based on the concept of Corenblit et al., (2015) *adapted by* Schwarz et al. (2018)

The conceptual model described in Figure 5, contains these 'stage-morphology' and but also the related 'feedbacks'. The development of the deflation basin and the depositional lobe for each stage and the abiotic and biotic processes to shift between the stages are shown in section A. In section B the governing feedback in each stage are given. These three stages can be associated with the three blowout stages; Initiation, development and closure (described in sections 2.2.1 – 2.2.3).

In the geomorphological stage, the blowout will be initiated. The initiation is mainly driven by the erosional sediment transport processes leading to an increased width and depth over the blowout deflation basin. The width to depth ratio is increased and this will decrease the plant biomass. Erosion will continue and erosion tolerant species start to colonize which decreases the wind speed.

When the abiotic processes are reduced relatively, the vegetation recolonizes along the deflation basin and the depositional lobe. The abiotic and biotic processes start to interact in the bio-geomorphologic stage. Herein the interaction between the blowout morphology, sand transport, substrate and plant specifications plays an important role. Due to the increased vegetation and therefore induced sand accumulation, the deflation basin will close. This is the start of the ecological phase which is determined by the growth of vegetation and reduced physical disturbances.

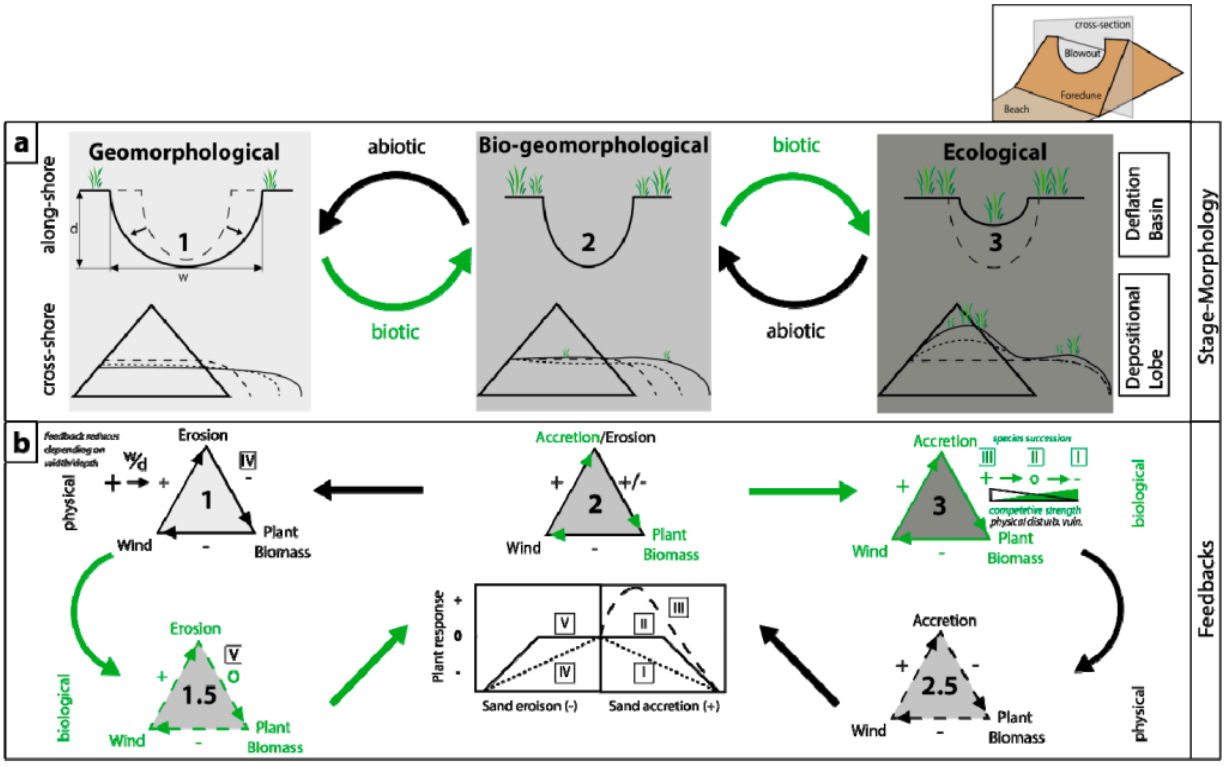

Figure 5 a) Conceptual model of the evolution of the deflation basin and the depositional lobe of a blowout in the three successional stages; Geomorphological stage, bio-geomorphological stage and ecological stage. b) The feedback mechanisms on the blowout evolution in the different stages (Schwarz et al., 2018).

2.3 Research question

This MSc research aims to improve the knowledge about the (bio)-geomorphic development of foredune blowouts by comparing different blowout sites on the long term. This is done by answering the following research questions focussing first on the morphological changes, secondly on the three-phase evolution depending on thresholds and lastly by explaining potential differences between the blowout sites.

1. What is the morphological change of each specific foredune blowout annually and seasonally?
   a. How does the blowout area change?
   b. How does the blowout volume change?
   c. How are the obtained changes in area and volume related?
2. How can we determine the three-stage evolution of a blowout (initiation, development and closure)?
   a. In what stage is the blowout? And how is this related to the changes in the area of sand and vegetation spatial?
   b. To what extent are thresholds between the various vegetated stages related to sand dynamics (erosion/deposition)?
3. Which factors determine the differences in development characteristics between each blowout site?

3. Study areas

In this research six blowout sites located along the Dutch coast are studied. Different blowout characteristics are represent at these six sites. For example, trough- or saucer morphology, the size including wind direction angles and if the blowout is connected to the beach or not. Also the ages and if the blowout is natural or man-made differ. In the case of man-made blowouts, the way in proceeding these features may differ as well. All six blowouts show similar and different characteristics between each other, so in that way the research questions can be solved.

Noordvoort (52° 19.803'N, 4° 29.814'E)
The site Noordvoort is a man-made blowout complex of approximately 0.05 km^2 (Figure 6). In 2013 the excavation of several notches into the foredunes started in order to restore a natural, gradual transition from the sea to the dunes. In addition, vegetation has been removed as part of Project Noordvoort initiated by Waternet. A blowout complex that is not connected to the beach, started to form.

Figure 6 Blowout Noordvoort source: Google Earth

Egmond-Bergen (52° 38.295'N, 4° 37.535'E)
The blowout site Egmond Bergen is located in Noordhollands Duinreservaat between the cities Egmond aan Zee and Bergen aan Zee (Figure 7). The study area is approximately 0.09 km^2. The back dunes consist of various small saucer blowouts but in this study the focus is on the large trough blowout which is connected to the beach. In 1998-1999 two depressions appeared that were not connected to the beach. In 2013 they were connected to the beach, and formed a trough blowout with two main lobes.

Figure 7 Blowout Egmond-Bergen source: Google Earth

Bloemendaal (52° 25.552'N, 4° 33.562'E)
The site of Bloemendaal is a study area of 0.4 km^2 located north of the city Bloemendaal aan Zee in National Park Zuid-Kennemerland (NPZK) (Figure 8). The blowout complex was initiated by excavating five different notches in the 20m high foredune around 2012-2013 during the Noordwest Natuurkern project. More landward, vegetation was also removed to create large areas of bare sand. The development of the notches from 2013 until 2016 was previously researched by Ruessink et. al (2018). The man-made notches are comparable to natural trough blowouts which are connected to the beach.

Figure 8 Blowout Bloemendaal source: Google Earth

Schouwen (51° 41.214'N, 3° 41.106'E)
With 0.9 km^2 Schouwen is the largest studied blowout complex located in the Natura 2000-area 'Kop van Schouwen' (Figure 9). It is the dune area in the western end of Schouwen Duivenland. Since 1995 the nature management authority Staatsbosbeheer intends to create a dynamic situation to restore the back dunes (Arens, 2014). In the projects 'Programmatische Aanpak Stikstof' (PAS) and 'Innovatief Nederlands Kustbeheer' (PINK) damages to the dunes after storm events are no longer repaired and the scheduled nourishments are passed for once. Small cuts in the foredune appeared but also in later years several blowouts started to form.

Figure 9 Blowout Schouwen source: Google Earth

Terschelling 1 (53° 24.579'N, 5° 18.635'E)
Two sites are located on the Dutch barrier island, Terschelling. The first site *Terschelling 1* is located on the north coast between Formerum and Hoorn with a study area of approximately 0.25 km^2 (Figure 10). The morphology of this coastal section is quite natural with probably a lot of sand transport transversely by looking at the JarkusRaai profiles (Arens et al., 2007). The blowout system was excavated and vegetation was removed in March 2019 by looking at the satellite imagery. Nowadays there is one large and several smaller artificially saucer blowouts which are not connected to the beach.

Figure 10 First blowout Terschelling source: Google Earth

Terschelling 2 (53° 22.810'N, 5° 11.102'E)
The second site of Terschelling is located on the north-western part of the beach shore between 3-4 km (Figure 11). The study area is approximately 0.165 km^2. There are two natural trough blowouts in a 24m NAP massive foredune which additionally developed in the past but they were closed several times to keep the foredune intact (Arens et al., 2007). Since 1995 the maintenance of the foredunes was reduced to maintain the coastline flexible. The trough blowouts are connected to the beach with a high opening of 6m NAP and a width of 10-15m.

Figure 11 Second blowout Terschelling source: Google Earth

4. Method

To give insight into the blowout changes on the long- and short-term, two datasets are used; PlanetScope multispectral satellite imagery and airborne LiDAR data. The PlanetScope data is almost daily available from 2016 – 2021 with a 3x3m resolution. These images are used to give insight into the annual and seasonal landcover changes. LiDAR elevation data from 2012 – 2021 with a resolution of 2x2m and 5x5m is used. This data is collected annually and thus only adequate to analyse the long-term annual elevation and volume changes. In this chapter, first the PlanetScope satellite image processing and analysing is discussed. Secondly, the LiDAR data processing and volumetric analysis.

4.1 PlanetScope

The PlanetScope satellite imagery is provided by the commercial company Planet. In 2016, the PlanetScope project launched Dove Classic satellites which came with a 4-band 'PS2' sensor with a ground sampling distance of about 3.7 m (Planet Labs Inc., 2021). They create daily multispectral 3x3m resolution imagery with four bands: blue (455–515 nm), green (500–590 nm), red (590–670 nm) and near-infrared (NIR) (780–860 nm) (Frazier & Hemingway, 2021).

The work flow for processing the PlanetScope data is shown in Figure 12. To find the suitable geospatial imagery, Planet Explorer is used. In this virtual environment, the imagery types 4-band PlanetScope Scene and RapidEye Orthofile are selected for the area of interest and the range of date is modified. To define the area of interest a GeoJson was created using *http://geojson.io*. The usability of the imagery depended on atmospheric disturbances such as clouds, shadows, and satellite flight paths. Merging of images was not necessary due to a large amount of almost daily imagery. If an image has been visually found suitable, it is clipped to the area of interest and the GEO tiffs are ready to download. 4-band PlanetScope Scene ortho scene imagery which is corrected for surface reflectance is used for the best analytic purposes. The default projection is in UTM WGS84/UTM zone 31N (EPSG 32631) which needed to be reprojected to the Rijksdriehoek coordinate system (RD_new EPSG 28992) for consistency with the different data sources. This is done with Gdalwarp simultaneously with correcting the pixel size to the precise 3x3m.

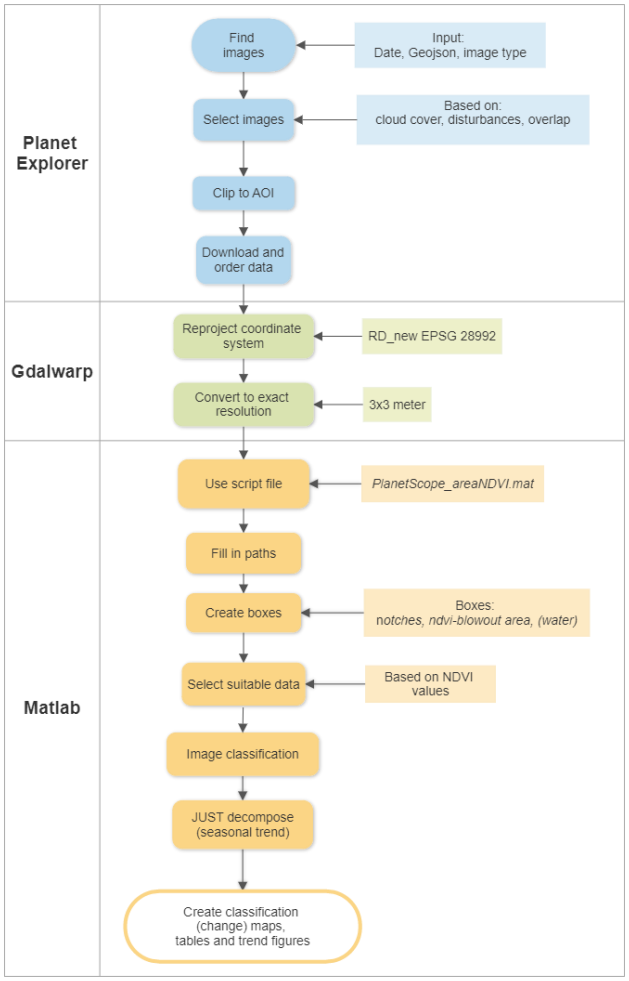

Figure 12 Work flow for deriving and processing the PlanetScope satellite imagery using the programs Planet Explorer, Gdalwarp and Matlab

The multispectral PlanetScope GeoTiff data is now ready to be used in the Normalized Difference Vegetation Index (NDVI) (Eq. 1). The NIR (Near Infrared) and Red bands are used for sand/vegetation separation by means of a NDVI analysis. This index compares the reflectivity of the red wavelengths bands (RED) of 0,66 µm and Near-Infrared radiance (NIR) with wavelength around 0.86 µm. This yields values that range from -1 to +1 with values around 0.1

indicating sand and values above 0.3 indicating vegetation. The greener the vegetation, during the growing season, the higher the NDVI value. From this a threshold value to differentiate sand from vegetation in the dune area of interest will be defined.

$$NDVI = \frac{NIR - RED}{NIR + RED} \quad (Eq. 1)$$

This classification between sand and vegetation is done in MATLAB using the script file *PlanetScope_areaSandNDVI* (provided by B.G. Ruessink). The extent is based on the NDVI thresholding resulting in the land pixels being classified into sand and vegetation. The products of the different steps are displayed in Figure 13. Starting with the visualization of the PlanetScope 3-band satellite image (Figure 13A). For each site, an analysis box around the blowout (ndvi-blowout box) is drawn to define the NDVI histogram and find the NDVI value of the sand and vegetation peak (Figure 13B). In this NDVI box, the sand peak near 0.1 (yellow arrow) is almost equal in height to the vegetation peak near 0.5 (green arrow) (Figure 13C). To exclude water peaks, the sea and lakes are not inside the analysis boxes of five six sites. One extra approach is taken for the blowouts of the site Bloemendaal which are surrounded by lakes. This which makes the NDVI classification more difficult and therefore the script *PlanetScope_makeWaterMasks_Bloemendaal* is used to exclude the water areas in the NDVI analysis (provided by B.G. Ruessink). The data with NDVI values that are not likely (probably due to shadows), are removed from the dataset. Classification maps were made using the NDVI threshold at the bottom of the valley between the sand and vegetation peak (≈ 0.25 at the red arrow in Figure 13C). For this image, pixels with a NDVI below 0.25 are determined as sand and pixels with a NDVI above 0.25 as vegetation. Finally the sand area in m^2 in a specified blowout box was determined by multiplying the number of sand pixels by the pixel area 3x3m (Figure 13D).

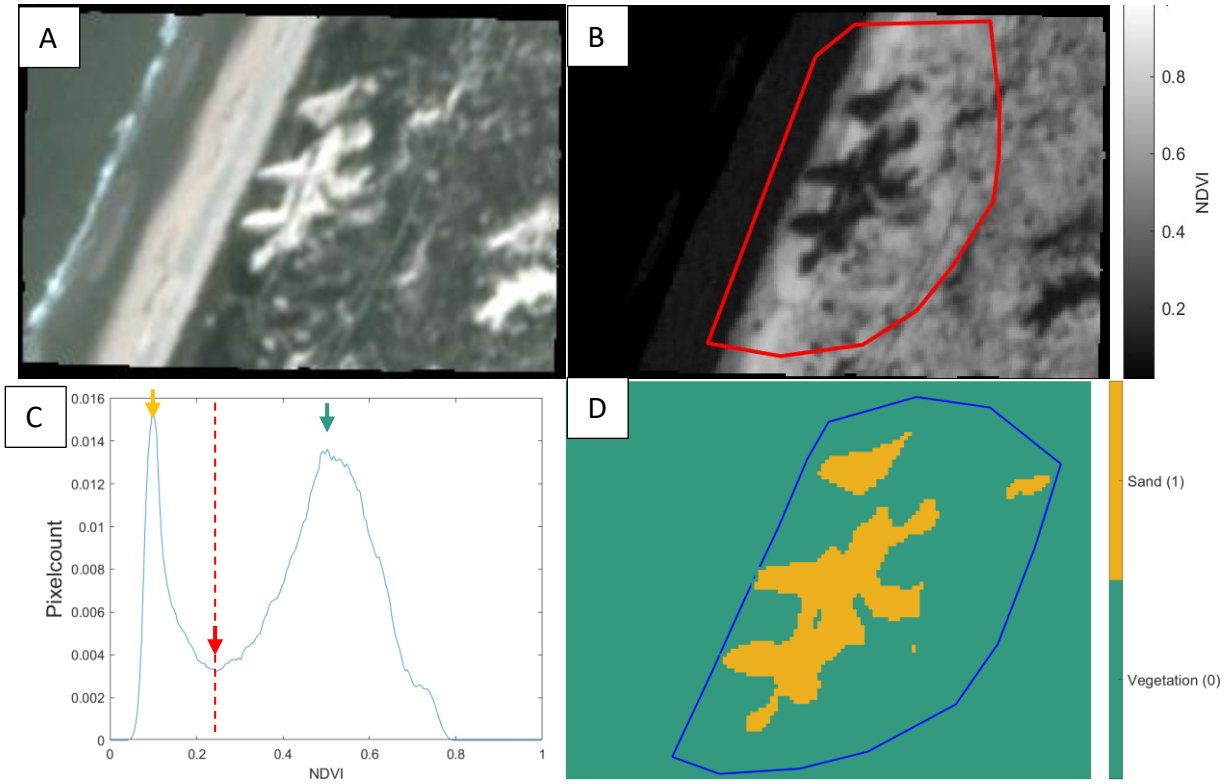

Figure 13 Work flow product of the site Noordvoort of 04-08-2020; A) Visual PlanetScope RGB image. B) NDVI map with the drawn NDVI blowout box (red). C) Distribution histogram of NDVI within the NDVI blowout box. (Yellow arrow -> sand peak, green arrow -> vegetation peak, red arrow and dotted line -> determined NDVI threshold in between the valley of the two peaks. D) Classification map with the blowout box (blue) wherein the sand areas were determined. Classification outside the blue blowout box is not relevant to the analysis.

The time series derived from the NDVI to monitor vegetation and sand dynamics were containing trends and seasonal variations. However, these time series consisted of abrupt changes in the trend and were not equally spaced in time due to the uncertainties and availability of the satellite imagery and the weather conditions. Therefore a method JUST (Jumps upon spectrum and trend) has been used to detect changes within unequally spaced time series and estimate the trend and seasonal components (Ghaderpour, 2021). The default settings given by *Ghaderpour* (2021) were used as the input parameters because they worked fine for the time series.

4.2 LiDAR

Airborne LiDAR elevation data was used to determine the morphological and eventually the volumetric changes. Since 1996 topographic data of the entire Dutch coast is annually collected in March with the airborne LIDAR surveys (Bochev-Van der Burgh L. M. et al., 2011). They were commissioned by the Dutch governmental organization Rijkswaterstaat and carried out by commercial contractors. Digital Elevation Maps (DEM) with a spatial resolution of 5x5m or 2x2m are provided publicly. The coordinate system was given in RD new (EPSG 28992) and the resolution of all year data was converted to exactly 2x2m resolution with Gdalwarp. The DEMs from 2012 to 2021 were used for each site except for the site *Schouwen* where DEMs from 2016 to 2021 were used. This is because the flight path of the planes along the coast didn't cover the whole blowout area landwards prior to 2016. The data was collected in medio March which is in line for the start of the growing season.

The DEMs were compared to create elevation change maps to see the elevation change (deposition and erosion) of the blowouts. Also transects parallel to the coast over the foredune and perpendicular to the beach over the blowout were used for the creation of 2D profiles to analyse the horizontal and vertical morphological development. The relative volumetric change, erosion and deposition, are calculated by multiplying the annual elevation changes by the pixel area of de LiDAR data (2x2m). For the cumulative volumetric change, the elevation changes relative to 2012 (for *Schouwen* 2016) were multiplied by the pixel area.

5. Results

In the results, the morphological changes of each site are given. The description of a site is divided into two main parts: Blowout area changes and the blowout volume changes. This is done annually for sand area and sand volume and only seasonally for the sand area. From this, the evolution of the blowout can be determined. The results of the first site *Noordvoort* are explained more in detail but the same reasoning is used for the other sites. The focus is on the similarities and differences in development characteristics between the blowout. Section 5.2 contains the figures mentioned in Section 5.1.

5.1 Morphological changes

5.1.1 Noordvoort

Annual area change

Figure 14A shows the sand area of the blowout including the calculated trend and seasonal variability. The sand area overall trend was increasing 27.6% from the begin of 2017 (10739 m^2) to the end of 2021 (14835 m^2) implying a general sand area gain of ~962 m^2/year. Over the last years, there is always been an increase in sand area and a coupled decrease in vegetation area. To visualize the annual change in the sand and/or vegetation area, five images each year in June were used. The data points of the summer satellite images are marked in the total time series of the dataset (Figure 14A). These five images were selected based on the representation of the trend of all the data points in that period of the year.

The NDVI classification maps of the oldest available satellite image (13-06-2017), the most recent available satellite image (07-06-2021) and a satellite image in between (2-7-2019) were used to present the area changes between 2017 - 2019 and between 2019 – 2021 (Figure 14B). Red and orange illustrate the gain in the sand area and blue and light blue illustrates the gain in the vegetation area. It is visible that gain in the sand area is especially seen at the three depositional lobes which have grown ~15 m/year landwards in northeast direction of the deflation basins. Also at the northern and southern edges of the three deflation basins there was an increase in the sand area. The change from sand to vegetation took place in between the different deflation basins and depositional lobes. On the whole, the change from vegetation to sand was far more pronounced than the reverse change, consistent with the trend in Figure 14A.

Seasonal area change

At the end of the growing season (September - November), the sand area was relatively low compared to the beginning of the growing season (February - March) where the sand area is highest (Figure 14A). The period with lower sand areas seemed to be more constant than the period with higher sand areas. The average difference between the largest and smallest sand area was 7646 m^2 in 2018, 7609 m^2 in 2019 and 7645 m^2 in 2020 which corresponds to 45%, 42% and 40% of the highest sand area. The years 2017 and 2021 were not taken in because winter month data was not available which will be further discussed in section 6.4. The maximum difference in landcover between the ending and beginning of the growing season of the year 2019 is shown in Figure 14C. Blue illustrates the change from sand to vegetation which dominated the change from vegetation to sand illustrated by red. The spatial change was located all around the edges of the blowout and the foredune.

Annual volume change

Figure 14D shows the elevation changes (delta Z in m) with the perimeter of the sand area in 2021 (red) and the two transects over the foredune and the blowouts (black). The three deflation basins eroded 4 to 10 m. The erosion was very concentrated compared to the deposition which was more spread out landwards. North-east of the deflation basins, the depositional lobes increased in height between 2 to 4 m while in between the deflation basins, the surface slightly increased in height by approximately 0.3 m. Also, sand is deposited outside perimeter which means that vegetated areas also increased in height.

In Figures 15E and 15F the 2D elevation change profile cross-sections over the foredune and over the southern blowout are shown. In 2013-2014 three notches were excavated, with a depth of 0.5 to 1.5 m. Over the years, the two artificially blowout deflation basins deepened 8 to 9 m till 2020 wherein the deflation basin stayed constant in height. The erosional walls started to increase in height about 0.5m in 2016 resulting in rim dunes. In the profile over the blowout the excavation in 2013-2014 and the deepening of the blowout are visible (Figure 15E). The blowout was not connected to the beach. The height change of the transition between the deflation basin and the depositional lobe stayed constant. In the year 2017-2018 the blowout deepened the most up to ~3.5 m, and the depositional lobe filled up two depressions with ~1 m of sand.

From the elevation data, the volumetric changes were calculated in a stated box around the blowout including sand and vegetated area. In 2013-2014 the excavation of the notches started which resulted in the large negative sand volume change (Figure 15G-H). From 2014-2015 erosion and deposition both increased, with deposition being slightly larger than erosion volume (Figure 15G). In later years, erosion actually exceeded deposition to some extent. In the year 2015-2016 considerably more sand was deposited while the erosion rate almost stayed the same. This resulted in a large positive sand

volume change with a cumulative increase of 3125 m^3 from 2015 -2018 which was ~1042 m^3/year (Figure 15I). In the following years, 2018-2021, the sand volume change was balanced more towards a negative change and therefore depletion with a cumulative sand decrease of 2306 m^3 or a decrease of ~769 m^3/year.

5.1.2 Egmond-Bergen

Annual area change

From med 2016 to med 2018 the sand area trend was increasing by 24.8% (~4922 m^2/year), from 2018 to 2019 the trend was decreasing by 16.0% (~5495 m^2/year) and from 2019 to 2021 the trend was increasing again by 27.5% (~ 6508 m^2/year) (Figure 16A). This was a net sand area increase of 17364 m^2 from 2016 (29924 m^2) to 2021 (47288 m^2) which corresponded with a change of 36.7% of the total sand area and an overall increase of ~3473 m^2/year. By looking at the spatial area change,both depositional lobes expanded (Figure 16B). The northern lobe expanded immensely on all sides over the last two years, while the eastern lobe expanded mainly at the edges of the lobe (~4 m/year) from 2017-2019 and at the end of the lobe (~17.5 m/year) from 2019-2021

Seasonal area change

Each year the seasonal area change was about ~10400 m^2/year which corresponds with a change of 23%, 24% and 25% of the highest sand area (Figure 16A). The peaks of the largest and smallest sand area were shifted one month each year. The spatial seasonal area change in 2018 was especially visible in the eastern lobe on which vegetation expanded considerably at the beginning of the growing season (Figure 16C). The northern lobe had seasonal sand area development at the edges of the lobe but also decreasing scattered areas of sand in the middle of the blowout. This resulted in patches of vegetation in the starting period of the growing season.

Annual volume change

From 2012 to 2021 the blowout developed erosion up to ~15 m at the deflation basin and deposition up ~9 m at the two depositional lobes (Figure 17D). In the erosion area, there were three areas parallel to each other, which merged at their landward site where the erosion was largest. Also, the back dunes showed a slight increase in height.

The 2D elevation profile over the foredune shows that ~8 m of sand eroded in 2012 – 2015, which resulted in one wider southern deflation basin (Figure 17E). More northwards there was less wider basin with steeper walls. Over the years both deflation basins increased in width and in depth. In Figure 17F a higher area close to the foredune with a depression in the middle is shown. From 2012 to 2021 this higher area lowered by 13 m in total and flattened out landwards, showing the change from the initial saucer high on the foredune to a trough blowout connected to the beach. This resulted in a 4 m raised depositional lobe with landward grow of ~13.5 m/year. Also, the foot of the foredune elevated ~1 m since 2015. The latter is also visible in Figure 15D as alongshore continuous deposition on the upper beach. This presumably reflects the built-up of a row of incipient dunes.

Each year the total annual volume was increasing but did not show a clear trend (Figure 17H). Each year more deposition took place except for the year 2020-2021 when there was a net balance between deposition and erosion (Figure 17G). The cumulative volume change from 2012 - 2021 showed a total increase of ~3.5×10^4 m^3 sand, implying a sand volume increase of ~0.38×10^4 m^3/year (Figure 17I). The positive sand budget suggests a net import of beach sand throughout the years.

5.1.3 Bloemendaal

Annual area change

An overall positive trend of 15.0% is presented from the end of 2016 (126963 m^2) to the end of 2021 (149391 m^2) which is a sand area gain of 22428 m^2 in about five years implying a sand area increase of ~4486 m^2/year (Figure 18A). The spatial increase of sand area appeared mainly at the depositional lobes in the north-eastern direction and at the foredunes (Figure 18B). On the northern side of the deflation basins and depositional lobes the sand area increased more relative to the southern side. This happened in 2017-2019 as well as in 2019-2021.

Seasonal area change

A clear seasonal variability with steep peaks for large areas of sand and less steep valleys for smaller areas of sand is visible (Figure 18A). The seasonal fluctuations had its largest sand areas around March and its smallest sand areas around November (2018) and August (2019, 2020) (Figure 18A). The seasonal variation fluctuated between an average of 33000 m^2/year or 20-22% a year on the total maximum area of sand. The seasonal change from sand to vegetation in 2019 was present all around the edges of the blowout, especially at the two most southern lobes (Figure 18C).

Annual volume change

The erosion and deposition patterns from 2012 to 2021 are shown in Figure 19D. All the five notches eroded up to 14 m. Also, two small areas of erosion appeared north of the two southern lobes, on the parabola dunes that in the winter of 2012/2013 have been cleared of vegetation. Sand was deposited on all lobes, especially at the two most northern lobes which were more stretched out landwards. This deposition reached 9 m. Outside the sand area perimeter, there were no notable height changes.

In the profiles over the foredune and over the blowout, the excavation in the year 2012-2013 is visible (Figure 19E-F). The excavation of the second notch (deepened ~3 m) (seen from the south) was not as deep as the other notches (deepened ~18 m) (Figure 19E). The five deflation basins of the blowout showed a different development in width and height. For example, the second deflation basin showed more changes in depth than in width, while the forth deflation basin showed changes in depth and also in width. In between the deflation basins sand was deposited as rim dunes of up to 3 m. In the profile over the second blowout (from the north) showed the excavation of ~7 m in the foredune. Afterward the deflation basin eroded by a few meters, whereby a depositional lobe grey landwards 19 m/year and thereby filled up the existing depressions by 2 meters of sand.

In 2013 relative to 2012 a large amount of sand volume was excavated resulting in a negative total annual volume (Figure 19G-H). In 2013-2014 the erosion volume was still slightly higher than the deposition volume (Figure 19G). From 2014 on, the deposition volume exceeded the erosion volume, resulting in a positive sand budget with a cumulative increase of ~0,7 x 10^5 m^3 implying a sand increase of ~1x10^4 m^3/year (Figure 19I).

5.1.4 Schouwen

Annual area change

Over the years there is a positive trend of 40.9% in the sand area resulting in a total sand area gain of 100846 m^2 from the end of 2016 (145.888 m^2) to the end of 2021 (246.734 m^2) which is a general sand area increase of ~20169 m^2/year (Figure 20A). Each year the blowout area expanded except for the year 2020-2021. The sand area especially expanded with a northern lobe in the years 2017-2019 (Figure 20B). Further, there were no distinct depositional lobes since the blowout is very complex and

big in size. In the northern part of the study area, there was a transition of from sand to vegetation but on the whole this was not so pronounced as the change from vegetation to sand.

Seasonal area change

The sand areas were fluctuating seasonally (Figure 20A), with the largest areas, at the beginning of the growing season, in April. At the end of the growing season, in September, the areas of sand were the smallest. Each year the seasonal variation in landcover was around ~62000 m^2 which was 25%, 27% and 30% of the highest total sand area. The spatial area change in 2018 occurred at the edges of the blowout, with some larger parts in the northern lobes (Figure 20C).

Annual volume change

The elevation change between 2016 to 2021 is shown in Figure 20D. Close to the foredune parallel to the shore, erosion took place. Several deflation basins have evolved with erosion up to ~12 m. Sand was deposited on several lobes, especially landward of the wider basins. These lobes increased in height up to ~7 m but since the blowout is very complex, this value varies substantially in alongshore direction. Inside the sand area perimeter of 2021, large areas also showed almost no height changes. The same applied for the back dunes landward of the perimeter.

In the 2D profile over a part of the foredune from 2016-2020 showed the development of a southern 10-m-deep blowout (Figure 21E). It has deepened ~1.5 m/year to a total deepening of 7 m and expanded ~5 m/year further to the north over the years. North in the transect, two depressions developed and expanded to the north. The most northern part of the foredune stayed constant in height except for the year 2020-2021 when some erosion took place. The 2D profile over the southern 10-m deep blowout showed the connection to the beach over the years (Figure 21F). The foredune eroded from 18.5 to 8 m while a lobe expanded landwards by ~17 m/year. Especially in the year 2020-2021, a large amount of sand was deposited at the lobe which even reach a height change of 13.5 m.

From 2016 to 2017 there was more erosion resulting in a negative sand volume change (Figure 21G-H). In the years 2017-2018 and 2018-2019 the deposition exceeded the erosion resulting in positive sand volume change. In 2019, 2020 and 2021 the sand volume change was negative again due to the high erosion volumes. The cumulative sand volume respectively to 2016 increased of ~4.4 x10^4 m^3 from 2017-2019 implying a sand volume increase of ~2.2x10^4 m^3/year. In the years 2019-2021 the cumulative sand volume decreased ~4.6 x10^4 m^3 implying a decrease of ~2.3x10^4 m^3/year (Figure 21I).

5.1.5 Terschelling 1

Annual area change

The first notch of *Terschelling 1* was only recently excavated, hence there are only results from 2019 to 2021. Figure 22A presents that the sand area was increasing 26952 m^2 from 2019 (70924 m^2) to 2021 (97876 m^2) which corresponds to 27.5%. This is was sand are gain of ~8984 m^2/year. The spatial area change between 2019 and 2021 shows that the blowout expanded all around the edges and became more connected to the beach (Figure 22B).

Seasonal area change

The seasonal variability had relatively steep peaks and more constant valleys (Figure 22A). The large sand area peaks occurred in April and the small sand area valleys occurred in August. In 2019 the seasonal variation was 18352 m^2 and in 2020 26205 m^2, which was respectively 21% and 27% of the highest sand area. The seasonal change in landcover in 2019 occurred around the edges of the sand area, mainly seawards (Figure 22C).

Annual volume change

The deflation basins of the blowout eroded up to ~2 m and the embryo dunes eroded even up to ~3 m in the years 2019 and 2020 (Figure 22D). At relative smaller areas, especially between the embryo dunes, sand is deposited up to ~3 m. Outside the sand are perimeter, little sand is deposited in the back dunes.

In the profile over the foredune one deep deflation basin with almost no elevation changes over the years is shown (Figure 23E). At the smaller deflation basins sand eroded up to ~2 m. In the transect over the blowout (Figure 23F), the excavation in the year 2019-2020 of ~0.5-1.5 m was visible at the north-western and south-eastern higher parts of the area. In the next year ~0.5 m sand eroded only at the north-western side. In between the higher areas, the surface is 8 m lower and not much has changed there. Landwards ~0.8 m of sand was deposited at the lobe in the year 2020-2021.

Since 2019 the sand budget changed from positive to negative (Figure 23H). Over the past years 2019-2021 both erosion and deposition volumes increased (Figure 23G). Every year the erosion exceeded the deposition which resulted in a negative cumulative sand volume change of ~0.97 $x10^4$ m^3 from 2019-2021 which was ~0.485 $x10^4$ m^3/year (Figure 23I).

5.1.6 Terschelling 2

Annual area change

Figure 24A shows a positive trend of 15.3%, which was a total increase of 13645 m^2 from 2016 (75527 m^2) to 2021 (89172 m^2) and a general sand gain of ~2729 m^2/year. The spatial development of the blowout happened mainly at the edges of the blowout system in the year 2017-2019 (Figure 24B). The blowout consisted of two main deflation basins with three depositional lobes of which the northern lobe showed the biggest increase in the sand area (~22 m/year) , especially from 2019 to 2021. In the total study period, the change from sand to vegetation took place in between the two other southern lobes. However the change from vegetation to change at the depositional lobes of the blowout was far more pronounced.

Seasonal area change

The seasonal fluctuations showed sand area peaks in May which was decreasing slightly in the following months but still remained constantly high till September (Figure 24A). In November the blowout sand areas were the smallest. The seasonal fluctuation was ~26.000 m^2 each year, which was 27%, 29% and 30% of the highest sand area. The spatial seasonal change for 2020 was visible all around the edges of the blowout, except for the northern lobe (Figure 24C).

Annual volume change

The elevation change is especially visible at the deflation basins and their depositional lobes (Figure 24D). The northern deflation basin eroded about ~15 m and the southern deflation basin eroded about 11 m. The three depositional lobes all increased in height elevated ranging from 3 to 9 m. The location where the blowout is connected to the beach and in between the deflation basins showed almost no height changes. Also outside of the perimeter no distinct elevation changes were found.

The previous results are also visible in 2D profiles over the foredune and the northern blowout (Figure 25E-F). Over the years two deflation basins eroded up to 4 to 5 m deep. The widening of both basins happened only on the northern erosion wall whereby large rim dunes formed (~3 m high). The northern deflation basin eroded gradually up to 2~ m/year (Figure 25F). The whole elevation profile flattened out in the landward direction which resulted in the formation of a steep depositional lobe.

The erosion volumes increased over the years until 2020 when they decreased (Figure 25G). The deposition volumes varied more and therefore determined the annual sand volume changes (Figure 25H). Each year the annual sand volume change is positive except for the years 2018-2019. From 2012 to 2021 there was a cumulative sand volume change of ~6x10^4 m^3 implying an increase of ~0.67x10^4 m^3/year (Figure 25I).

5.2 Figure sheets

5.2.1 Noordvoort

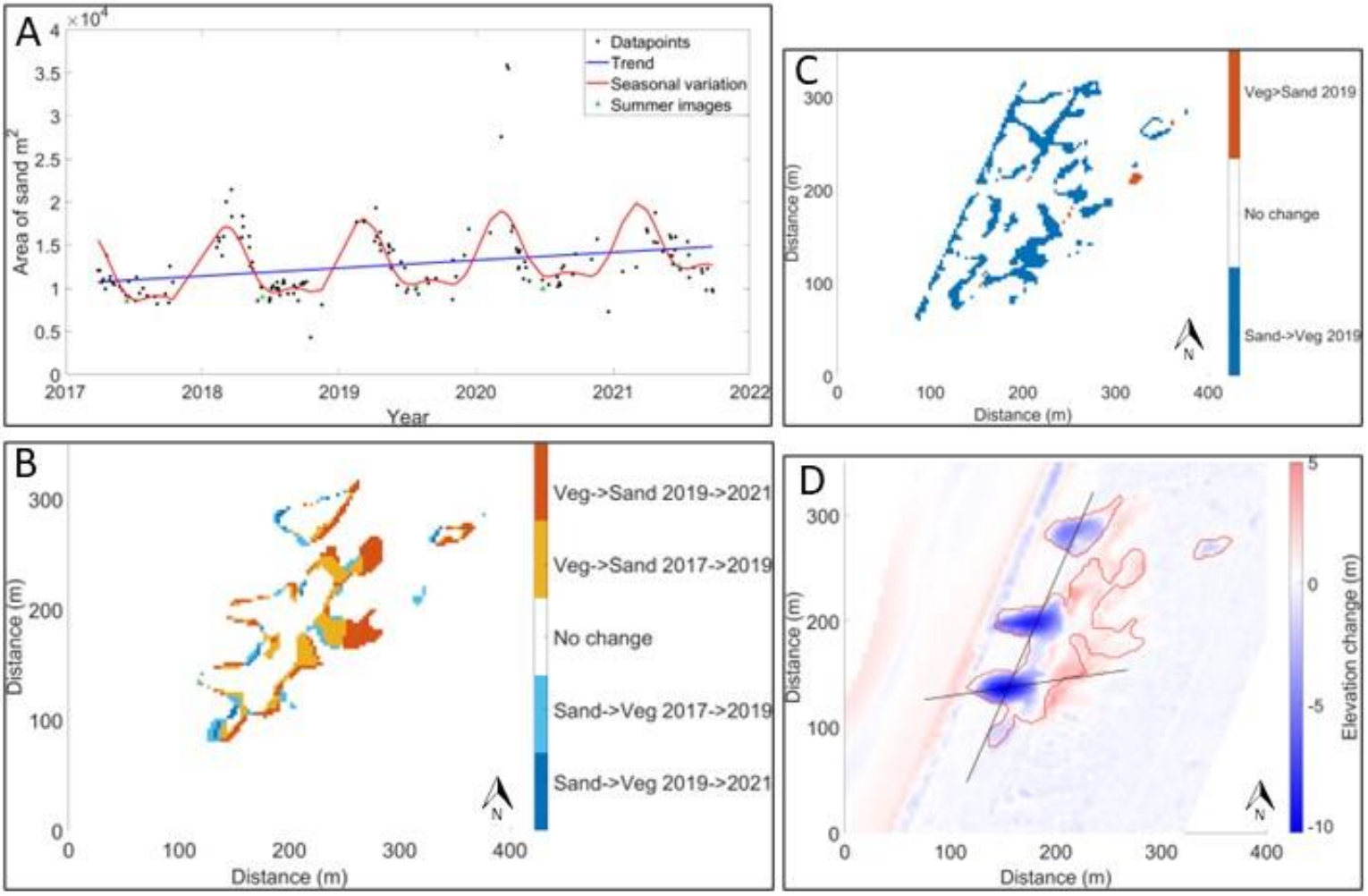

Figure 14 A) Sand area time series with trend and seasonal variations including summer images indications. B) Landcover changes between 2017-2019-2021. C) Seasonal variation spatial map of 2019. D) Elevation change map 2012-2021 with foredune and blowout transect and sand area 2021 perimeter

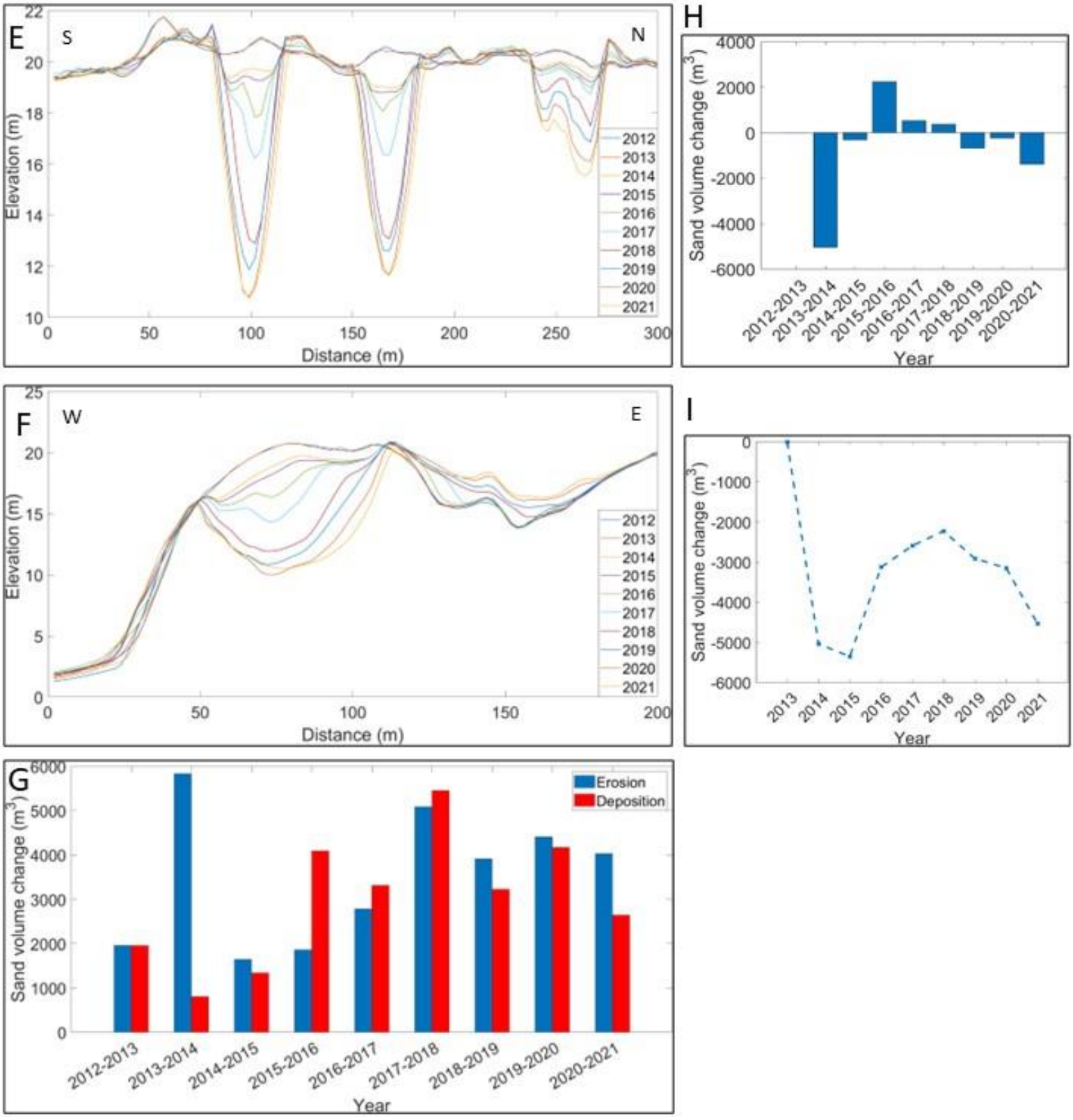

Figure 15 E) 2D elevation profile over the foredune. F) 2D elevation profile over the blowout. G) Deposition and erosion annual volume change in m³. H) Annual net volume change of sand budget in m³ I) Cumulative volume change respectively to 2012 in m³

5.2.2 Egmond-Bergen

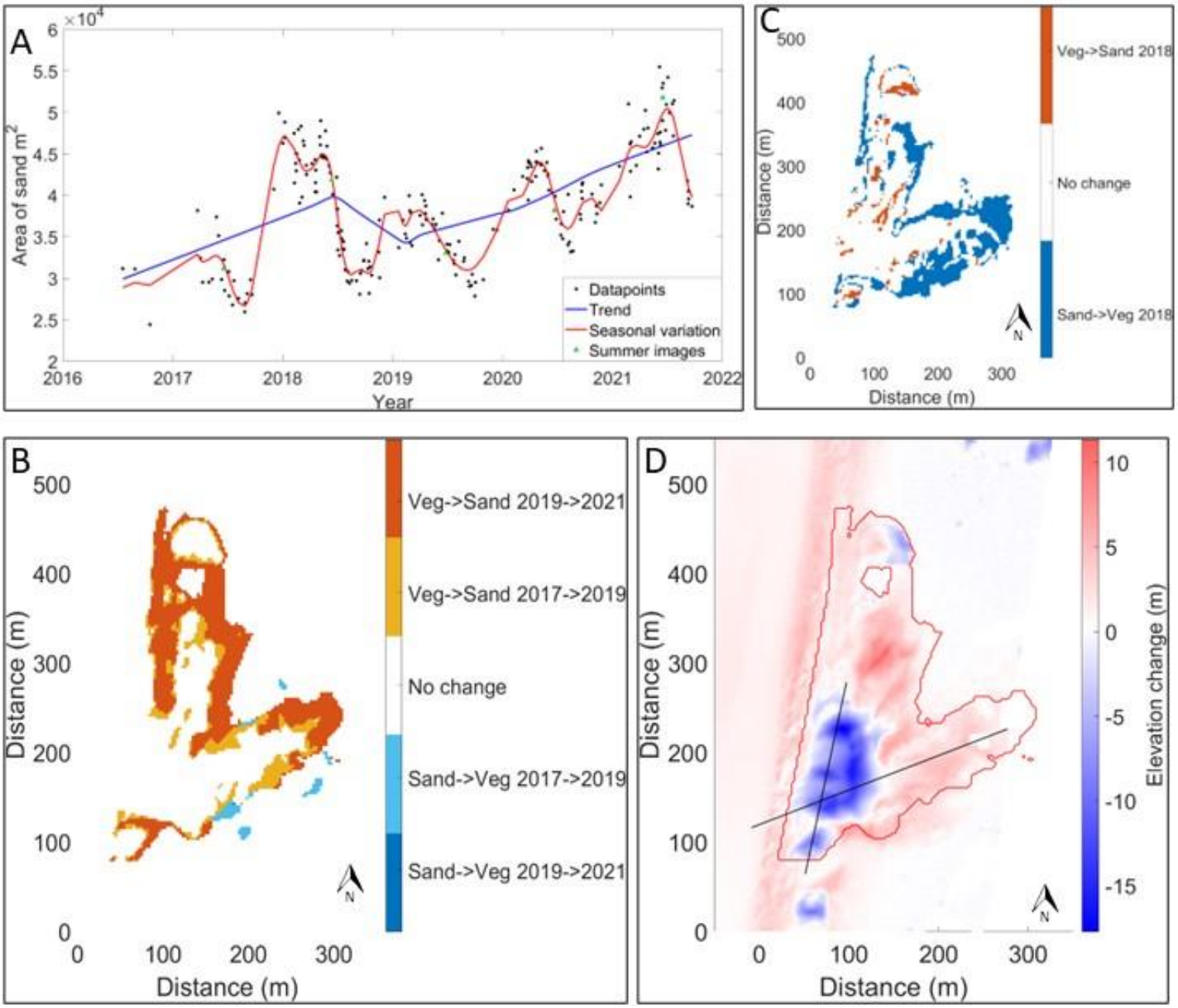

Figure 16 A) Sand area time series with trend and seasonal variations including summer images indications. B) Landcover changes between 2017-2019-2021. C) Seasonal variation spatial map of 2019. D) Elevation change map 2012-2021 with foredune and blowout transect and sand area 2021 perimeter.

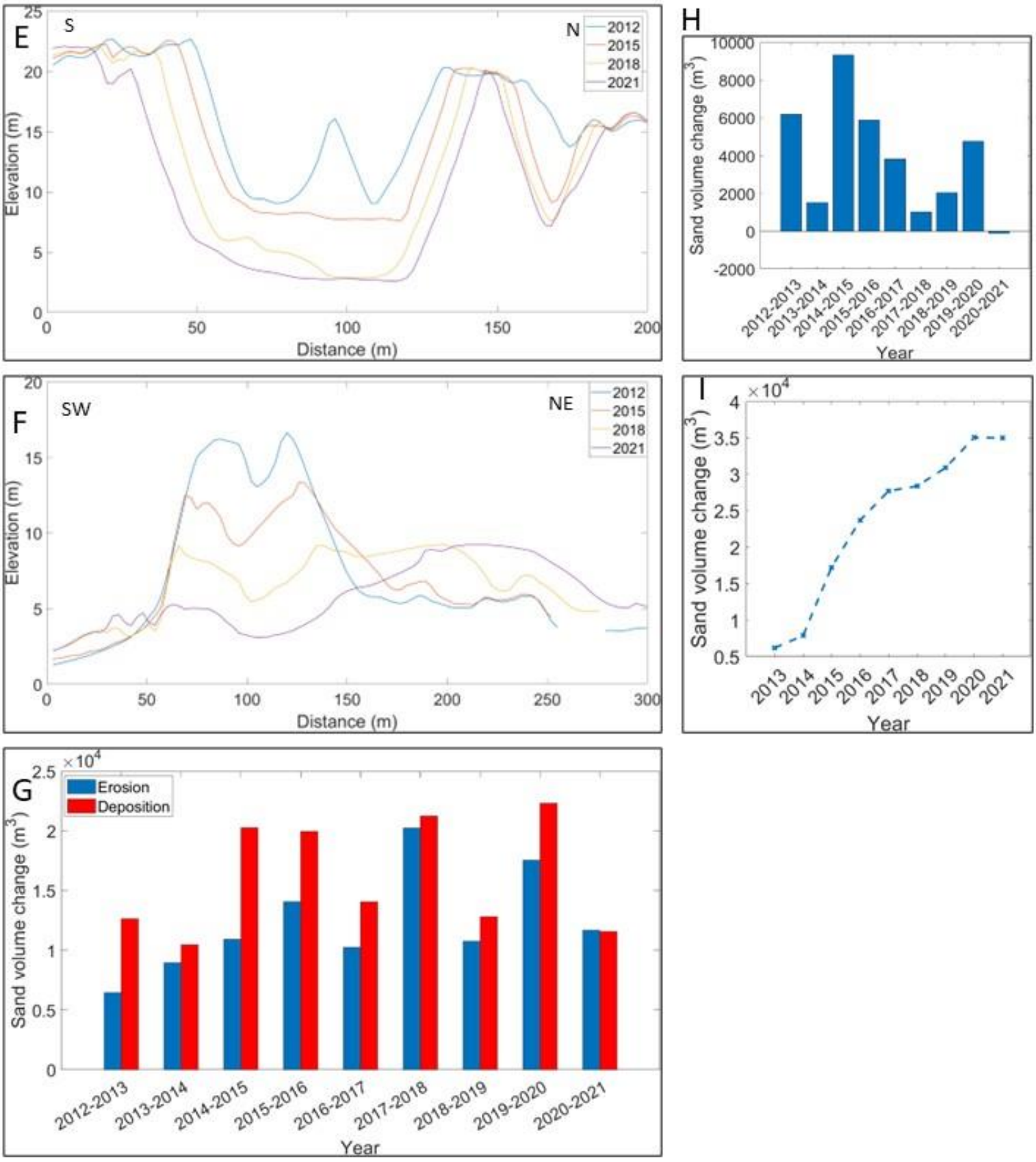

Figure 17 E) 2D elevation profile over the foredune. F) 2D elevation profile over the blowout. G) Deposition and erosion annual volume change in m³. H) Annual net volume change of sand budget in m³ I) Cumulative volume change respectively to 2012 in m³

5.2.3 Bloemendaal

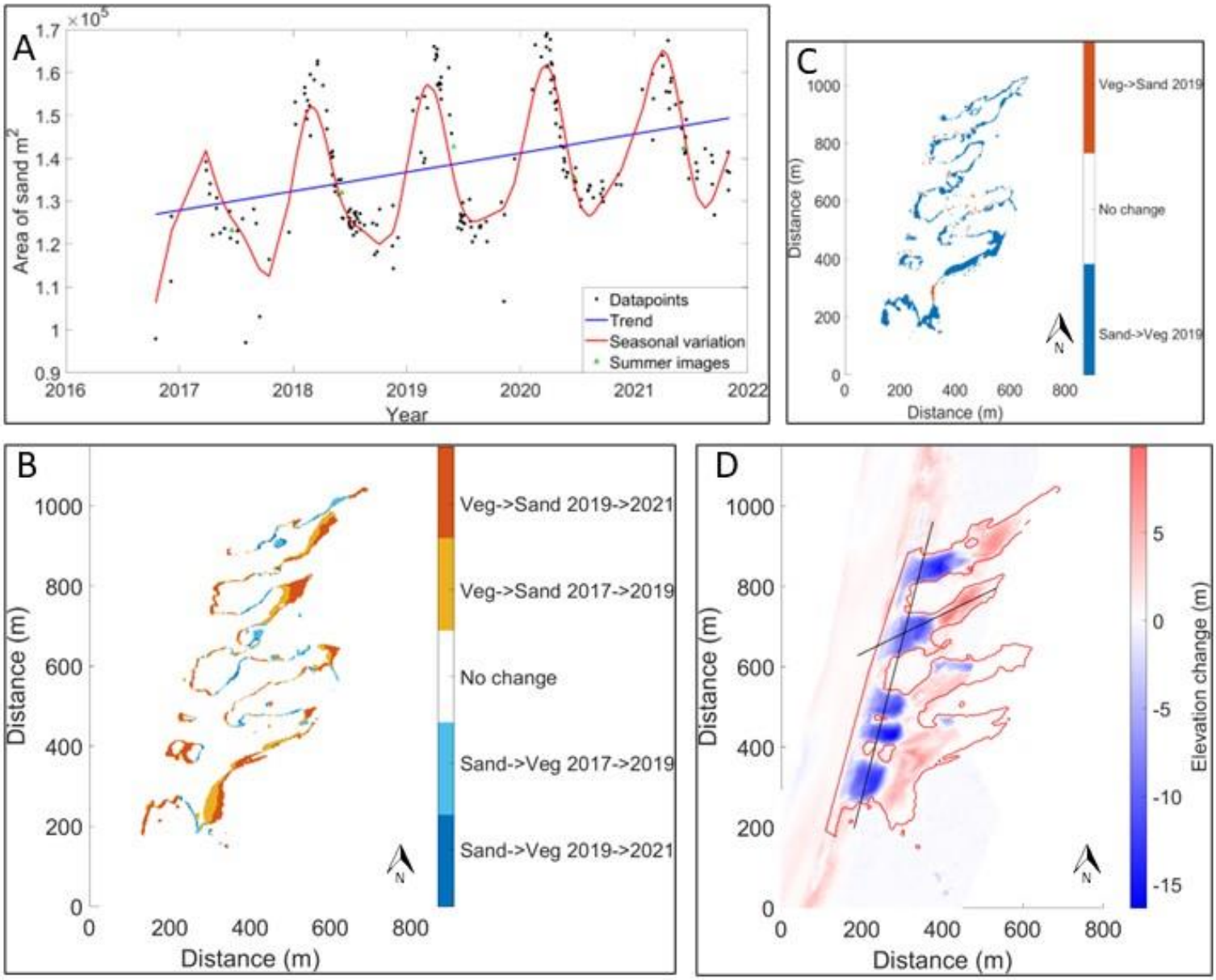

Figure 18 A) Sand area time series with trend and seasonal variations including summer images indications. B) Landcover changes between 2017-2019-2021. C) Seasonal variation spatial map of 2019. D) Elevation change map 2012-2021 with foredune and blowout transect and sand area 2021 perimeter.

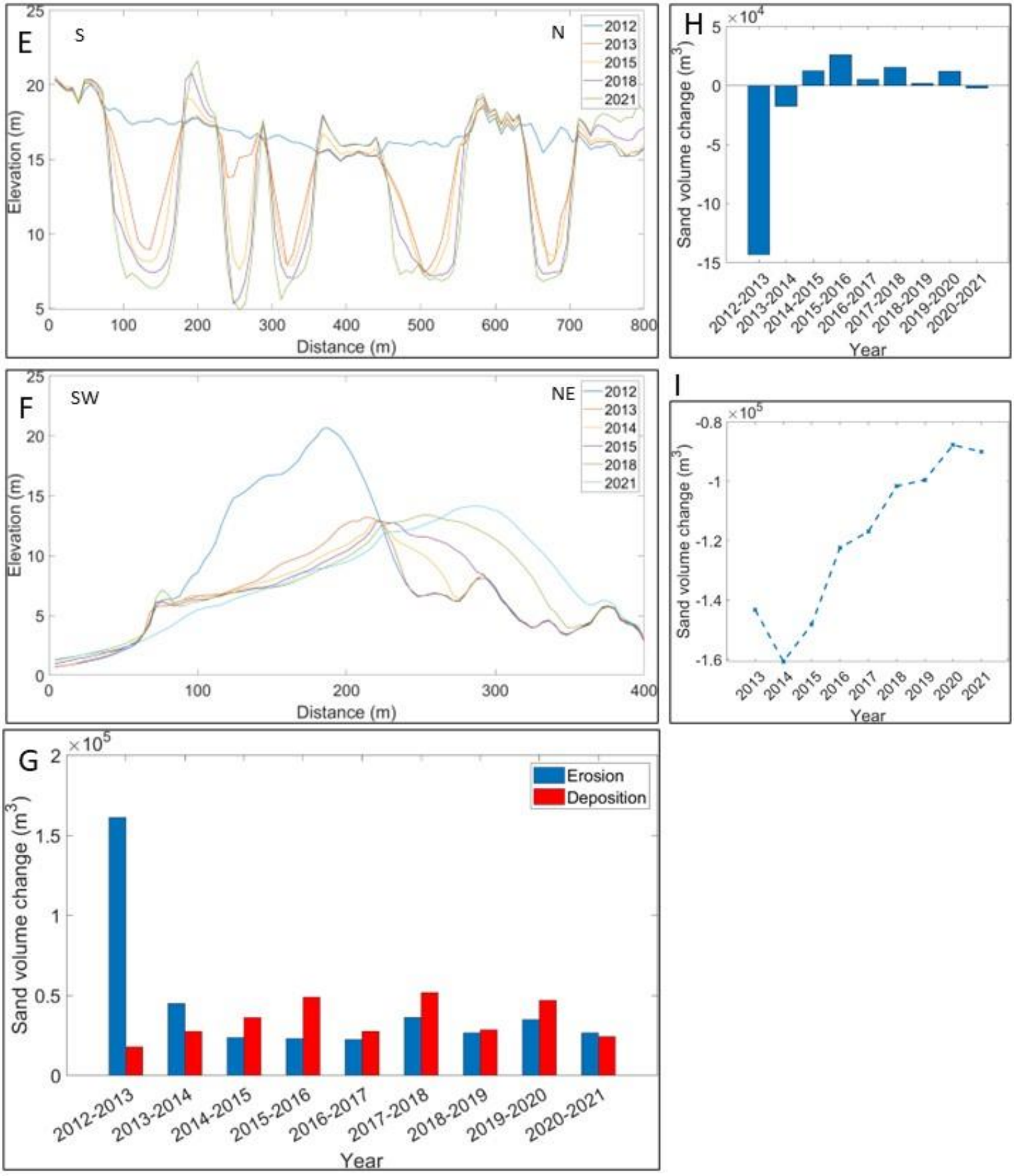

Figure 19 E) 2D elevation profile over the foredune. F) 2D elevation profile over the blowout. G) Deposition and erosion annual volume change in m^3. H) Annual net volume change of sand budget in m^3 I) Cumulative volume change respectively to 2012 in m^3

5.2.4 Schouwen

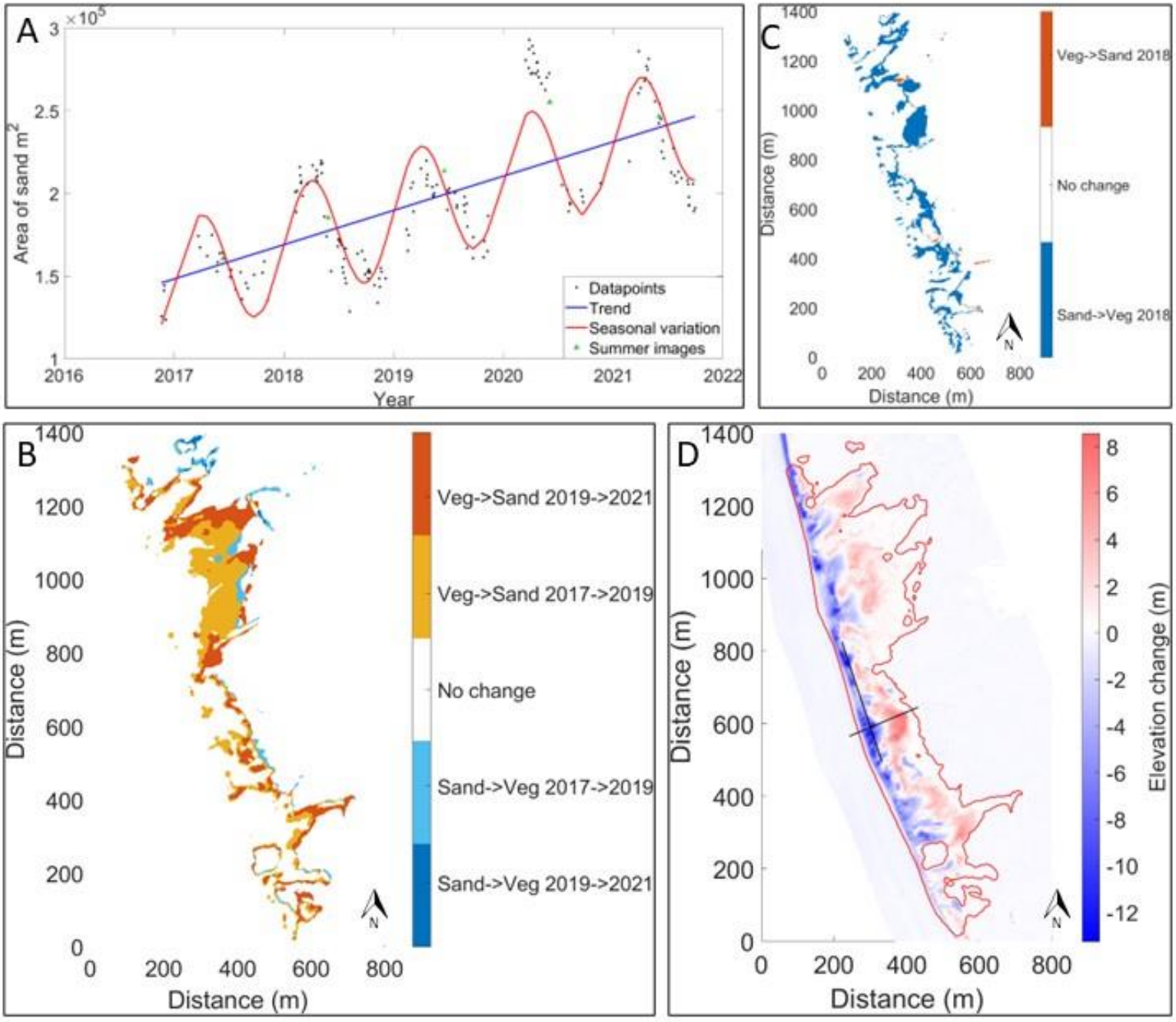

Figure 20 A) Sand area time series with trend and seasonal variations including summer images indications. B) Landcover changes between 2017-2019-2021. C) Seasonal variation spatial map of 2018. D) Elevation change map 2016-2021 with foredune and blowout transect and sand area 2021 perimeter.

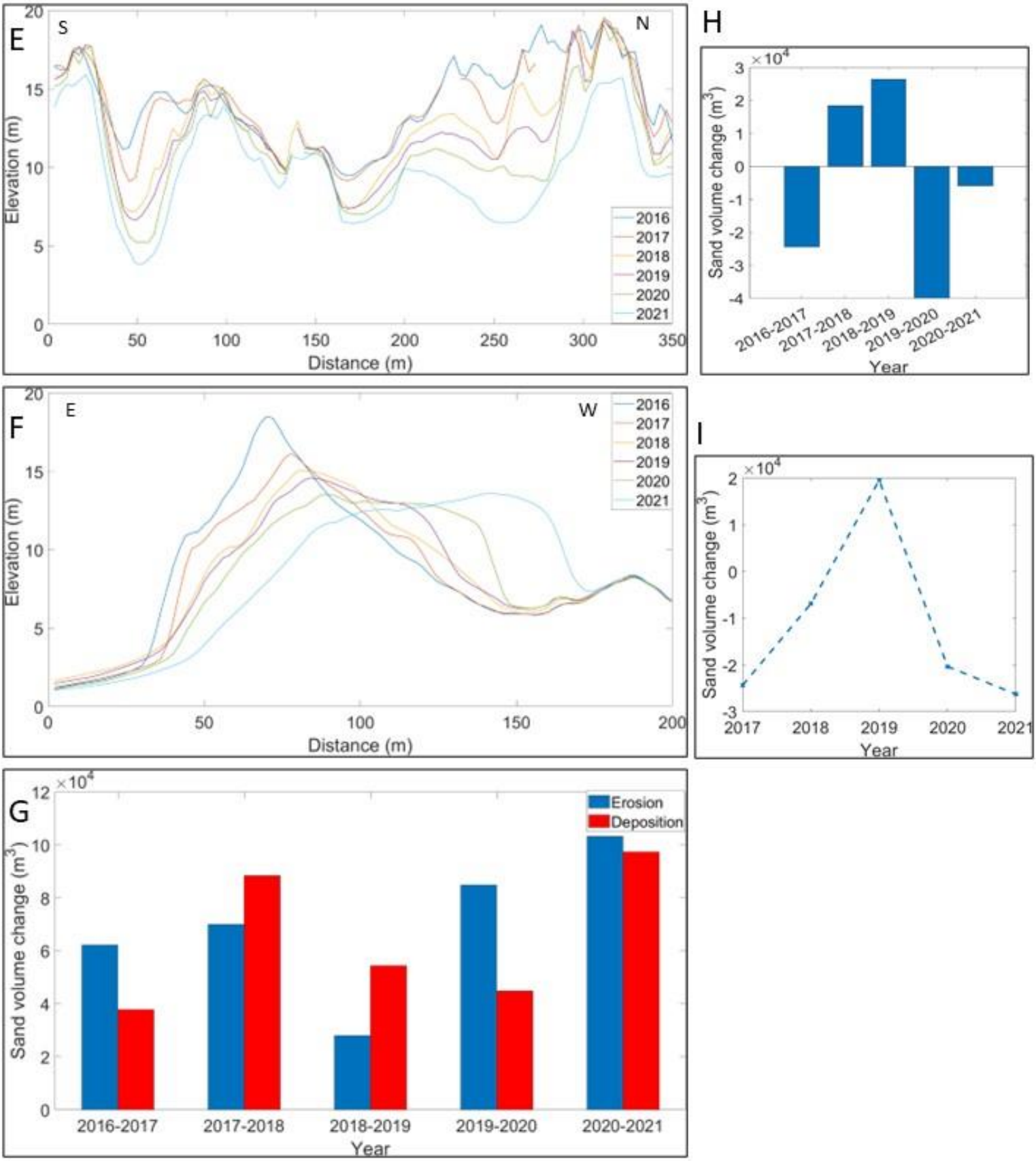

Figure 21 E) 2D elevation profile over the foredune. F) 2D elevation profile over the blowout. G) Deposition and erosion annual volume change in m^3. H) Annual net volume change of sand budget in m^3 I) Cumulative volume change respectively to 2016 in m^3

5.2.5 Terschelling 1

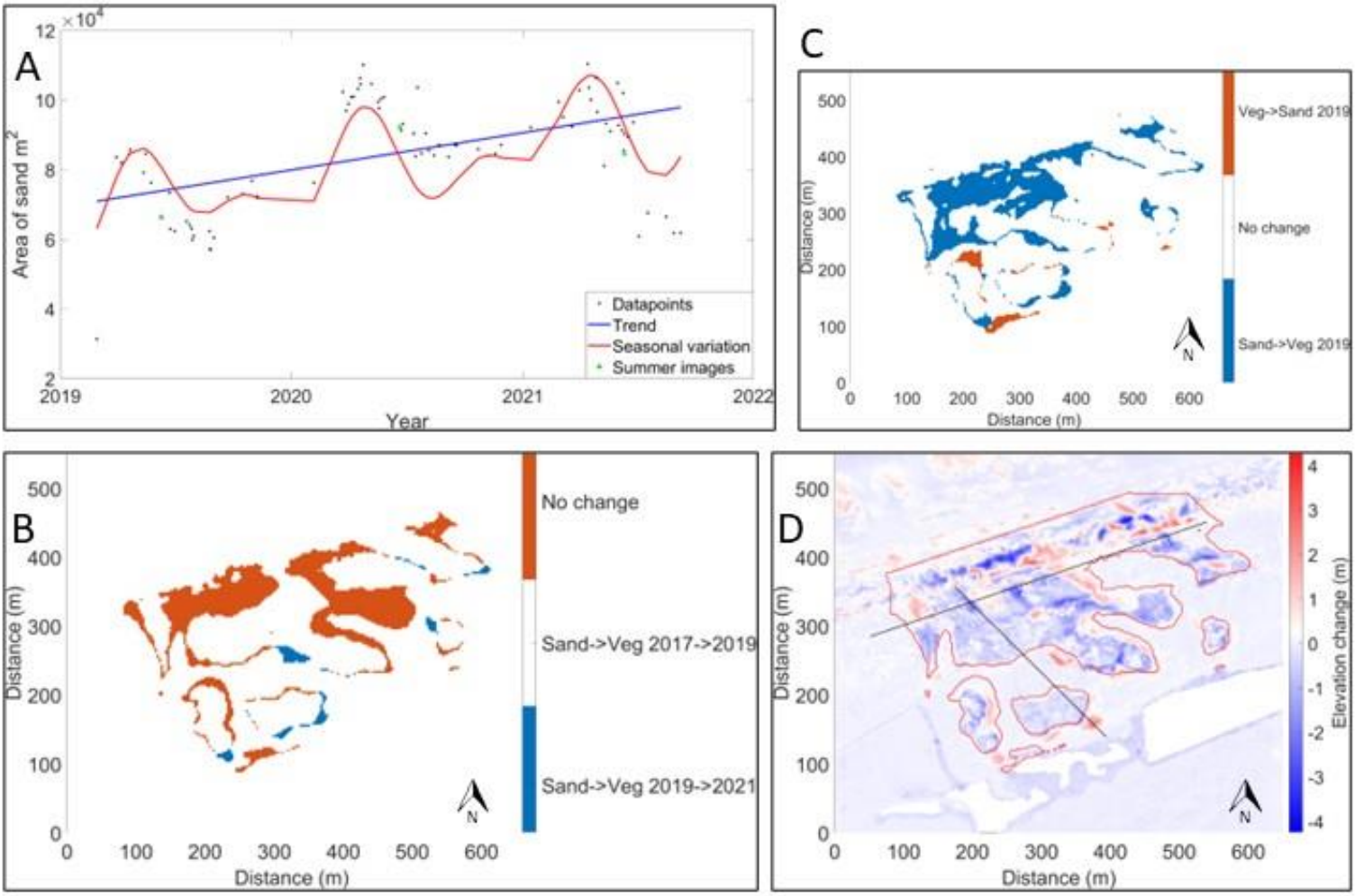

Figure 22 A)Sand area time series with trend and seasonal variations including summer images indications. B) Landcover changes between 2019-2021. C) Seasonal variation spatial map of 2018. D) Elevation change map 2019-2021 with foredune and blowout transect and sand area 2021 perimeter

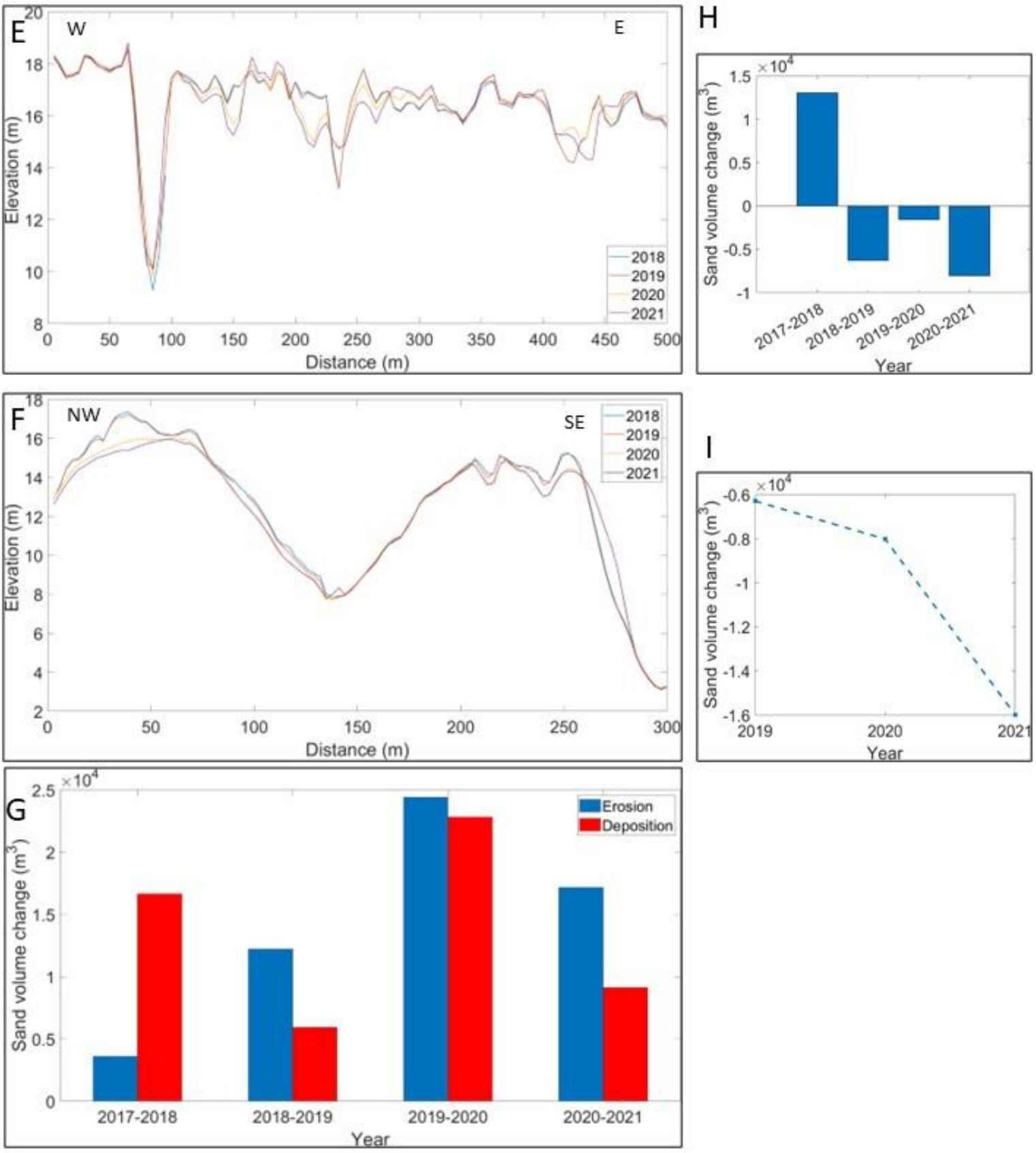

Figure 23 E) 2D elevation profile over the foredune. F) 2D elevation profile over the blowout. G) Deposition and erosion annual volume change in m^3. H) Annual net volume change of sand budget in m^3 I) Cumulative volume change respectively to 2018 in m^3

5.2.6 Terschelling 2

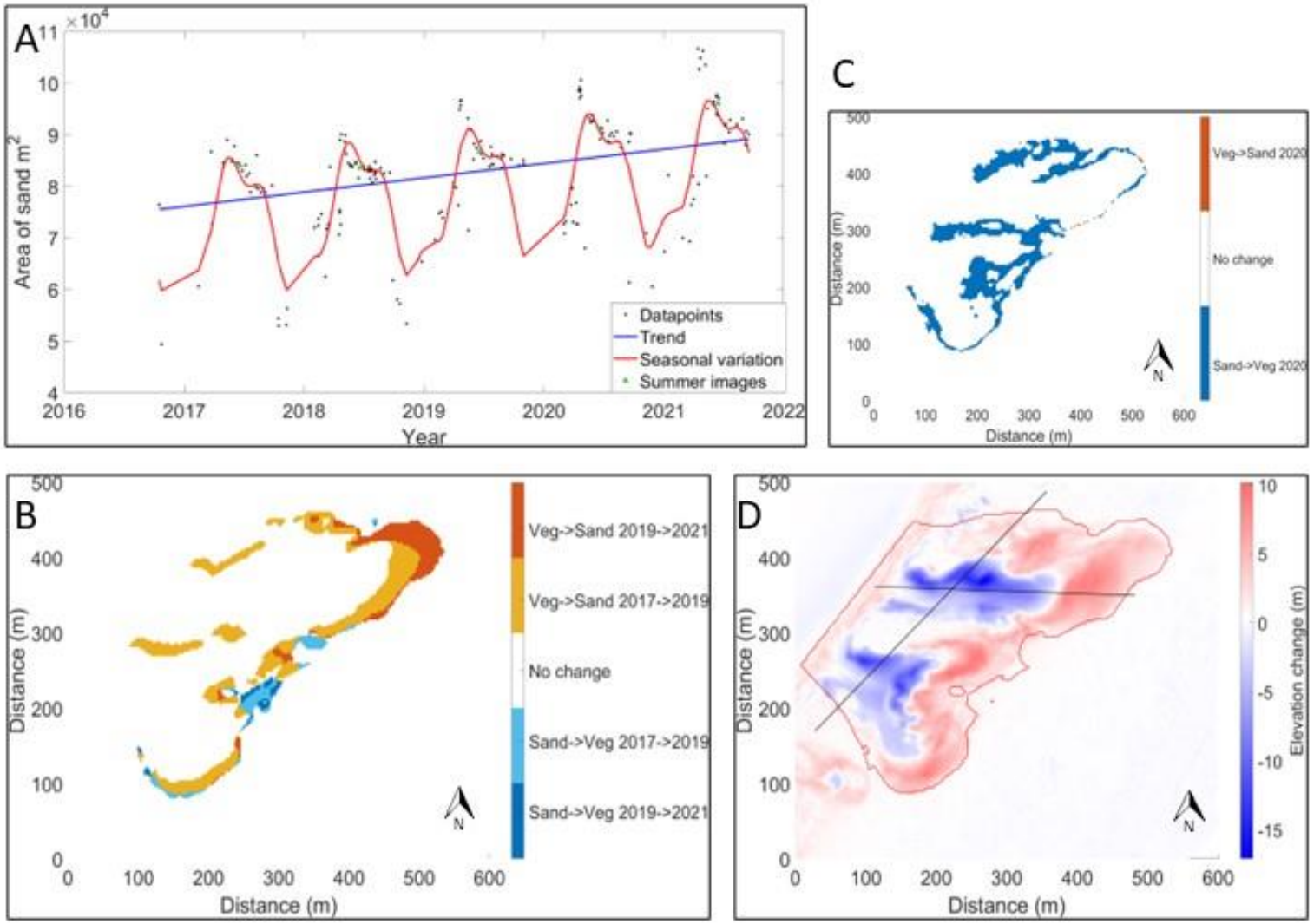

Figure 24 A) Sand area time series with trend and seasonal variations including summer images indications. B) Landcover changes between 2017-2019-2021. C) Seasonal variation spatial map of 2020. D) Elevation change map 2012-2021 with foredune and blowout transect and sand area 2021 perimeter.

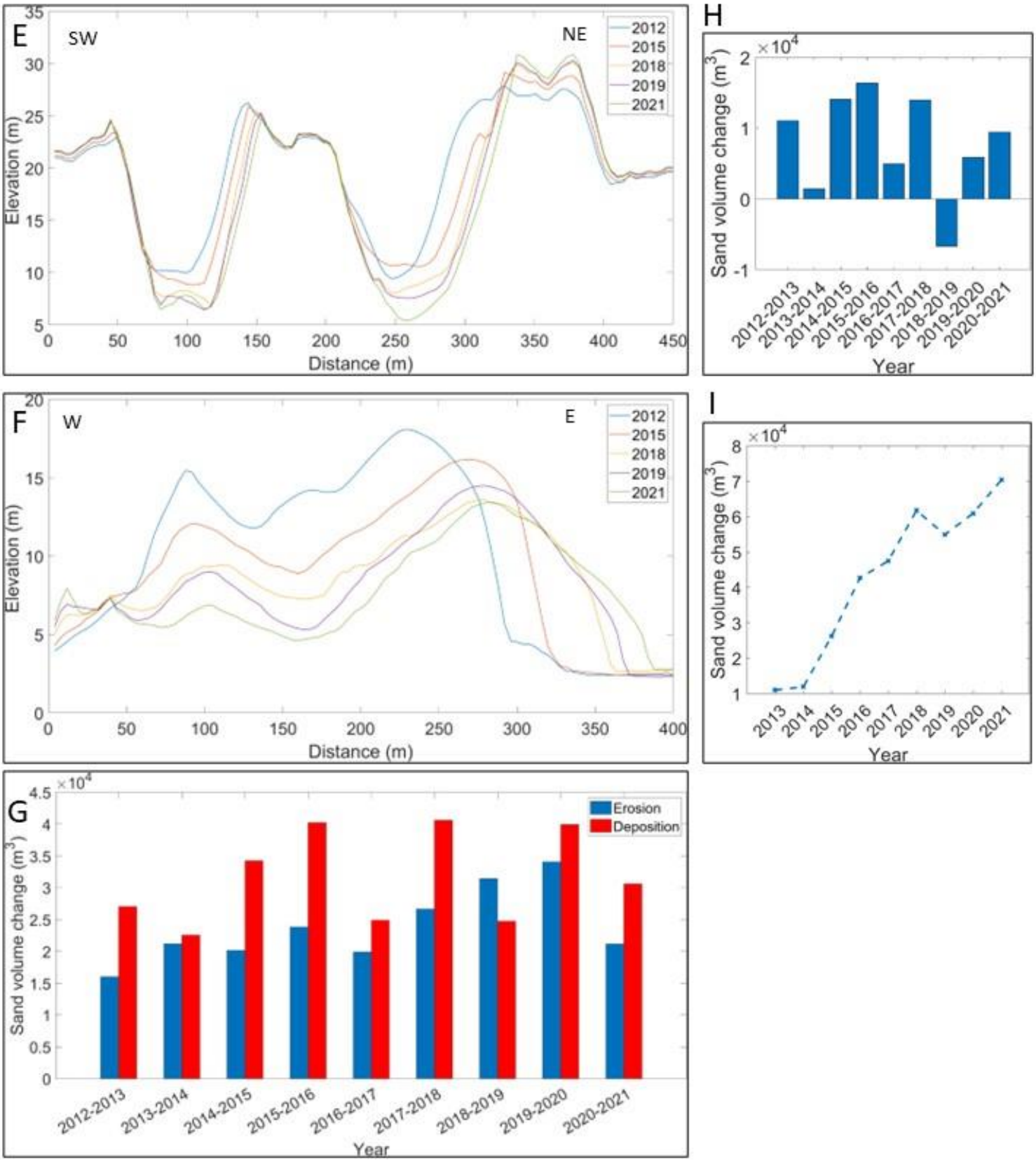

Figure 25 E) 2D elevation profile over the foredune. F) 2D elevation profile over the blowout. G) Deposition and erosion annual volume change in m³. H) Annual net volume change of sand budget in m³ I) Cumulative volume change respectively to 2012 in m³

6. Discussion

In this section the results for the individual blowout will be compared for areal changes, volumetric changes and how these co-vary. Figures from the figures sheet in section 5.2 will be combined as 'Figure A, B, C, .. etc." when preferential. Combining the two data sets couples the abiotic and biotic processes for the discussion about the blowout stage and transition in the development cycle. The discussion ends with possible errors and recommendations.

6.1 Blowout area change

6.1.1 Annual

Area trend

The overall trend for the sand area was positive at all the sites. In Figure 26 all the increasing trends and data points are plotted based on the size of the blowout. Also Figures A in the figure sheets shows the sand areas with the percentage of increase, based on the determined trend by JUST. The order of sand area increase from the end of 2016 to the beginning of 2021 is *Schouwen* (40.9%), *Egmond-Bergen* (36.2%), *Noordvoor*t (27.6%), *Terschelling 2* (15.3%) and *Bloemendaal* (15.0%). *Terschelling 1* was increasing 27.5% from 2019-2021. Implying that *Schouwen* expanded the most in blowout area.

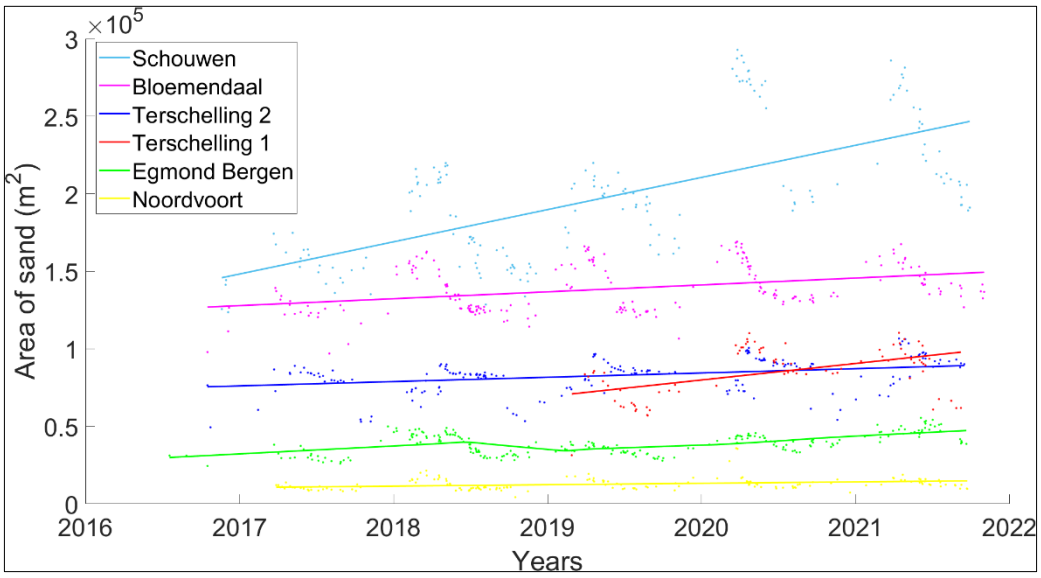

Figure 26 Comparison plot of the sand area in m² between 2016-2021 for all six sites including trend lines

Noticeable is the trend of *Egmond-Bergen* which was positive from 2016-2018 and from 2019-2020 but negative in the year 2018-2019. The same decrease in sand area was happening for the site of *Bloemendaal*. In the summer of 2019, there was more vegetation compared to the summer of 2018. The very dry summer of 2018 may have reduced the plant growth which may have resulted in less change from sand to vegetation in 2018.

Spatial

In Figures B the classification maps showed the development of the blowout. Only at a few locations, sand area persistently changed to vegetation area. This was in between different deflation basins and/or depositional lobes or scattered widely. The change from vegetation to sand was far more pronounced. The sand area gained at the edges of the blowout, especially at the depositional lobes in landward direction. At the edges the blowout, separation and deceleration of the wind flow occurs resulting in sand deposition and therefore lobe expansion landwards (Huggett, 2007).

Since the sand gain area was around the edges of the blowout, one may expect that the bigger the size of the blowout and therefore the larger the perimeter, the bigger the possibility for blowout expansion. Consequently larger blowouts may have more freedom for movement and incoherent have more deflation basins and depositional lobes. In that case, the largest blowout size of *Schouwen* corresponds with its sand area increment. *Bloemendaal* was also relative large in size but had not as much sand area gain as other relative smaller sites. Also the other blowout systems which more of less had the same size (~450 x 500 m) and exist of ~2 depositional lobes, showed different trends. So, overall size and relative increment are not strongly related by looking at these results.

At *Schouwen* and *Terschelling 1*, the sand area gain occurred especially all around the blowout edges while at the other sites, *Noordvoort, Egmond-Bergen, Bloemendaal* and *Terschelling 2,* the sand area grew mainly at the depositional lobes. The larger size and freedom of movement of *Schouwen* and the saucer blowout shape of *Terschelling 1* could be a reason for this overall blowout expansion. While at the other site the distinct deflation basins and the distinct depositional lobes grew as trough blowouts (Hesp, 2002; Huggett, 2007). This lead to distinct lobe growth of between 5 and 20 m/year which will be further discussed in section 6.2.

Due to the new Dutch coastal management, additions for a more dynamic dune system were established as mentioned in the Introduction. Different additions for each man-made blowout site, discussed in section 3, led to different blowout evolutions. For example, the man-made blowout Egmond-*Bergen* became connected to the beach in 2013 due to human interference and from then on its behaviour changed from a saucer blowout to a trough blowout (Figure 17F). Though the connection to the beach is not always created in the case of a man-made blowout. *Noordvoort* and *Terschelling 1* were man-made but are not connected to the beach. The man-made blowout, *Bloemendaal*¸ is connected to the beach and showed relative less sand area expansion than *Noordvoort*. Both are man-made blowouts established in 2013 with distinct depositional lobes but differ in connection to the beach. One may expect that a connection to beach lead to more aeolian sand transport originated from the beach, but in this example we saw that no connection can lead to relative more sand area gain. Other natural blowouts that had a wide connection to the beach, *Egmond-Bergen,* showed an even larger sand area gain. So, no strong relation with the beach connection which may drive the sand area increment difference was found. Overall more research could be done on the different human induced additions and their effects on longer timescales. The used satellite imagery obtained no data from the earlier years wherein most additions took place.

6.1.2 Seasonal

Figure 27 compares the seasonal variation between the sites. The data points of the seasonal fluctuations in the winter months were most of the time missing because the satellite imagery was not always available. This will be further discussed in the possible error in section 6.4. The date of the peaks with the highest and lowest sand areas differed somewhat for each site. The maximum sand area peaks were found in the months of March, April and May. The minimum sand area peaks spreaded more but were mainly found in September, October and November. Nevertheless, the peaks could be determined at the beginning and at the ending of the growing season. The period wherein the sand area was increasing and decreasing corresponds with the growth cycle of the vegetation. In autumn the vegetation is losing its green cover resulting in more identified sand pixels. In spring the opposite happens, resulting in more identified vegetation pixels. Especially for the site *Noordvoort* wherein the seasonal fluctuations remained constant in a low sand area which meant that the maximum vegetation cover period was longer. Also, that is why the lowest sand area peak was found in July which is early

in the year compared to the other sites. However, *Noordvoort* still had the largest change in seasonal landcover which can be explained by the large landcover change of the foredune as can be seen in Figure 14C.

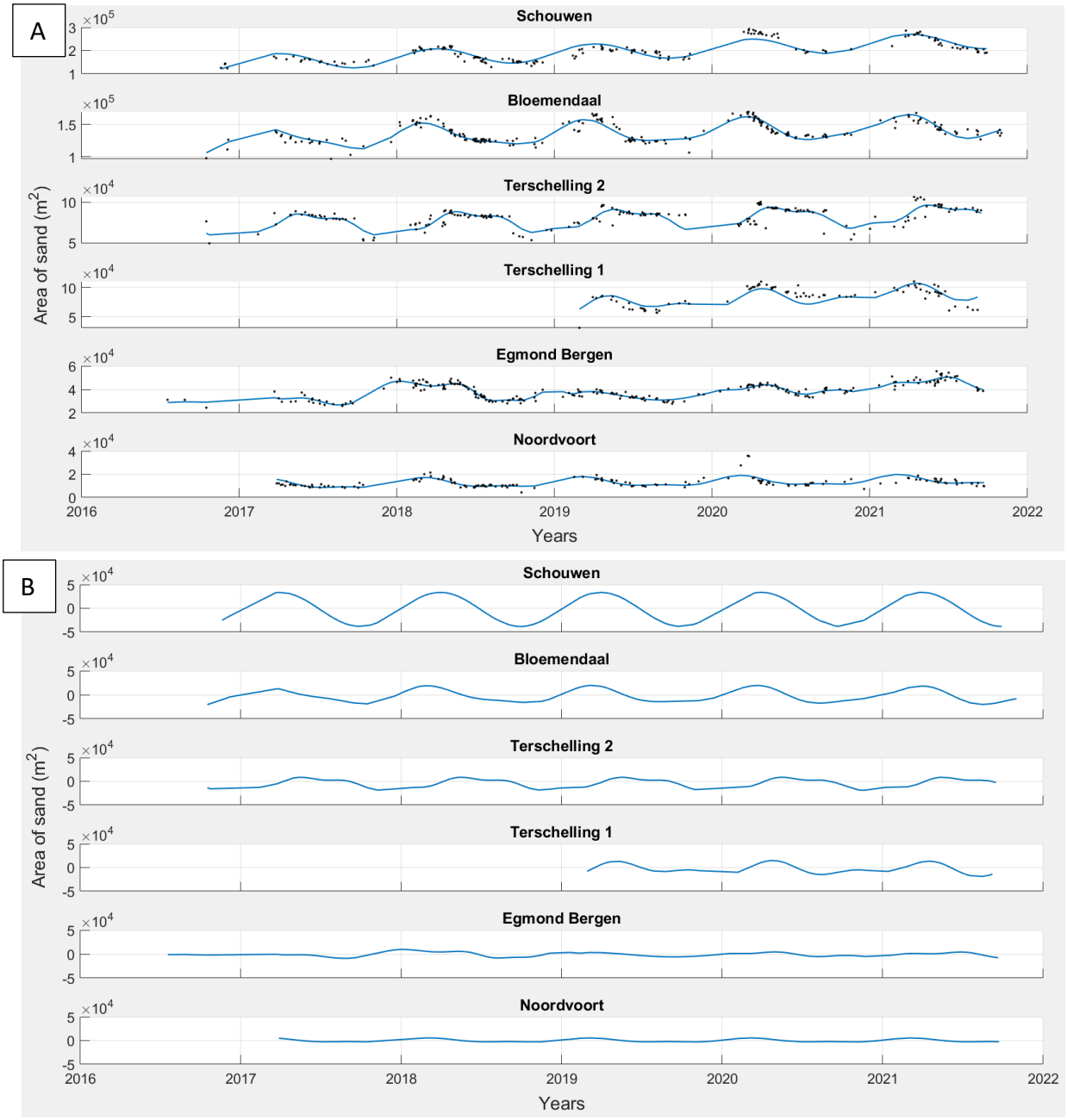

Figure 27 A) Seasonal variation in sand area + data point trend comparison of all six blowout sites B) Seasonal variation in sand area comparison of all six blowout sites

Spatial

In Figures C the spatial seasonal change is shown. At each blowout site, the alteration between sand to vegetation occurred around the edges of the blowout, especially around the depositional lobes. At the edges of the lobes, the layer of sand was thinner, which also can be seen in the 2D profiles in Figures F. On the thinner layer of sand, plant seeds were likely to germinate more or vegetation was not covered enough by sand and grew trough the layer again. The stable sand areas within the centre of the deflation basins (seen in Figures B) remained sand each year due to the high erosion rates (seen

in Figures D). *Schouwen* and *Bloemendaal* had the biggest distinct seasonal fluctuations in sand area (Figure 27). This could be explained by the large sizes of the two blowouts since the seasonal change was especially around the edges. At the sites of *Egmond-Bergen* and *Terschelling 2,* a relation between the seasonal and annual area changes was found. In the blowout lobes where the seasonal change was larger, the annual change was relatively less and where the annual change was larger, the seasonal change was relatively less.

6.2 Blowout volume change

The derived LiDAR elevation change maps as shown in Figures D, suggested that all the blowout sites have a dynamic activity due to the morphological changes. Volumetric changes were visible in the different blowout study sand areas while almost no changes were noticed in the vegetated back dunes. The locally increased erosion and deposition point out that the blowouts are dynamic.

Trends

Overall two trends in the sand volume were seen over the years for the different studied sites
The trends were analysed after excavations of the man-made blowouts which fall in the time span 2012-2021 of the elevation data.

1) First an increase in cumulative sand volume due to the positive sand budget. This was the case for the blowouts of *Egmond-Bergen, Bloemendaal* and *Terschelling 2*. *Egmond-Bergen* with a sand volume increase of $0.38x10^4$ m^3/year, Bloemendaal of $1x10^4$ m^3/year and *Terschelling 2* of $0.67x10^4$ m^3/year. The differences in these numbers are related to the size of the blowout and its increase in sand area. The positive annual volume change was present due to relatively more deposition than erosion. More deposition means that there must be sand originating from the beach, coming into the 'blowout box' through the blowouts. This positive sand budget means a net import of sand from to beach to the blowout. The sand is deposited on the depositional lobes which corresponds with the distinct lobe expansion of all three sites in the years 2017-2021 which will be discussed in section 6.3.

2) The second trend was an increase in cumulative sand volume followed by a decrease in cumulative sand volume for the sites *Noordvoort, Schouwen* and *Terschelling 1*. The sand volume of *Noordvoort* increased from 2015 on with ~$1.04x10^3$ m^3/year and decreased from 2018 on ~$0.77x10^3$ m^3/year. *Schouwen* increased in sand volume from 2017 on ~$2.2x10^4$ m^3/year and decreased from 2019 on ~$2.3x10^4$ m^3/year. This is related to the considerably more sand area gain in the years 2017-2019 respectively to 2019-2021, especially in the northern biggest depositional lobe (Figure 20B). For *Terschelling 1,* the sand volume increased only in 2018-2019 ~$1.75x10^4$ m^3/year and decreased from 2019 on ~$0.485x10^4$ m^3/year. Overall this trend corresponded with a positive sand budget followed by a negative sand budget while all blowouts showed an increase in sand area in the same time period (2017-2021). A negative sand budget, despite the relation between volume and area, could be explained by more erosion at the deflation basins, less sand input in the blowout system originating from the beach and a thinner layer of sand deposited landwards. This corresponded with the small height changes seen in the deposition lobes in 14D,20D and 22D in the last years.
Noordvoort and *Terschelling 1* are both man-made blowouts and not connected to beach. In the first years after the excavation the sand budget was positive probably due to the new initiation but in the years after the sand budget become negative. The missing connection to the beach might have limited sand input over time and ongoing erosion in the deflation basins exceeded deposition at the lobes. However, *Schouwen* had considerably more connections to the beach and showed the same volume trend. As well as the connection to the beach, the size and age of blowout did not influence the volume trend because all three blowouts differ in that aspect. Mentioning that indirect the size influence the only rates for sure.

Spatial

As can be seen in Figures D , the deflation basins decreased in volume while the depositional lobes increased in volume at every study site. The erosion in meters is much larger than the deposition in meters. The deepening and widening of the deflation basin happened at a relatively smaller area compared to the large deposition area at the lobes. These height changes happened mainly in the sand area perimeter. Outside the blowout complex, the back dunes elevated slightly but was almost negligible compared to inside the blowout complex.

In the cross-shore transects over the foredunes in Figure E it is seen that the blowouts deepened and widened over the years. At the sites *Noordvoort, Bloemendaal* and *Terschelling 2* typical rim dunes developed. In the transects over the blowout in Figure F, depositional lobe development and migration is shown. The negative elevation changes (erosion) were seen at the deflation basins and the positive elevation changes (deposition) at the lobes more landwards. This happened gradually for the sites *Egmond-Bergen, Schouwen and Terschelling 2*, whereby a landward migration of the blowout depositional lobe was noticed. The whole elevation profile flattened out in the landward direction whereby the lobes finally become higher than the initial deflation basins. All these blowouts behave like trough blowouts when connected to the beach. For the sites *Noordvoort and Bloemendaal*, a slightly different evolution was seen. The deflation basin of *Noordvoort*, which is not connected to the beach, was more deepened and depressions landwards were filled up with less lobe expansion. In Figure 14C-D it is seen that this depends on the transect over the blowout. In the most southern blowout less lobe expansion occurred. The site *Bloemendaal* was connected to the beach but showed a different profile. The deflation basin height stayed almost the same after excavation and the depositional lobe was expanding more. However, these findings still depend on the location of the transects over which blowout and so more transect are needed to improve this section.

In the profiles over the foredune (Figure E), the deepening and widening of the deflation basins showed indirect the erosional activity of the deflation basins of the blowouts. *Egmond-Bergen, Bloemendaal* and *Schouwen* were still very active with deepening of a few meters each year. *Noordvoort* and *Terschelling 2 s*eemed to reach the critical depth in the deflation basin because the deepening of the last two years was relatively small. A reason for this, for *Noordvoort,* could be the absent connection to the beach and the negative sand budget for the last years. The other blowout with no beach connection, *Terschelling 1,* is too young (initiation in 2019) to suggest its maximum erosion level. Another reason could be the maximum erosion for that blowout system and beginning of the transition to the bio-geomorphological stage. This may also be the case for *Terschelling 2*¸ which is a relative old blowout and may reach its maximum erosion earlier. However *Terschelling 2* was still increasing in sand volume and sand area in the last years (2019-2021) which contradicts the assumption. Therefore the oldest blowout, was still very active with the most blowout expansion each year. So no strong relations between the age of the studied blowout and their volume changes were seen.

Also, it is suggested that not all the sand was directly deposited at the connecting depositional lobes in the blowout sand area. This corresponded with the slightly elevated back dune areas that were visible for some study sites in Figures D. Some of the eroding sand emerging from the deflation basins was entrained in suspension and ended up in the back dunes. This again showed the contribution of the purpose to elevate the back dunes. It would be worthwhile to investigate the amounts that eroded related to the amounts that were deposited in the immediate vicinity and in the back dunes. More detailed maps of the back dunes and sand budget computations must be made in order to find out if there was induced accretion. Then by making the connection to a blowout type it can contribute to the vertical accretion of the back dunes with sea-level rise in mind.

6.3 Blowout stage

With the blowout area and volume changes the blowout stage can be determined following the conceptual model from Schwarz et. al. (2018)(Figure 5). At all sites, the deflation basins were still increasing in width and depth as a result of the abiotic processes. Also, most of the depositional lobes were still expanding landwards. These ongoing processes of aeolian sand transport would imply that all blowout sites were still in de geomorphological stage. At the sites *Schouwen* and *Terschelling 1*, there was a negative volume change over the last years, so more erosion relative to deposition. In the upcoming years, the lack of sand input and the erosion which exceed the deflation basin might encourage the change to the bio-geomorphological stage.

There were no suitable areas in the blowout complexes found, that would help to determine a threshold for the transition to a more bio-geomorphology or ecological stage. Nevertheless, a threshold that is related to the sand dynamics for possible transitions in the geomorphological stage might be determined. Therefore histograms were made that show the distribution of the height changes for the different landcover changes. This was done only for the site *Noordvoort* which had a distinctive expanding northern and southern lobe over the years 2017-2020 shown in Figure 28A. For each year a histogram was made for the northern lobe (Figure 28B) and southern lobe (Figure 28C). The PlanetScope satellite images to determine the landcover, were collected in June and the elevation data was collected in March. In this case, the landcover changes were analysed a few months after the height changes. This corresponds with the assumption that the vegetation changes are the effect of the sand dynamics related to the height changes. For example, if there is a lot of sand dynamics the lobe will expand.

In Figure 28A it is seen that the sand lobes were mainly expanding in the north-east direction. These pixels which indicated the change from vegetation to sand, had positive height changes up to even 2 m. For example, the southern lobe expanded considerably in 2018 with height changes between 0 to 1.6 m (Figure 28C). In these cases, enough sand was deposited at these pixel areas to initiated the landcover transition from vegetation to sand. However, the height changes were too spread for the different lobes and years to determine a specific deposition threshold for the transition from vegetation to sand. For the pixels that stayed sand, the height change was around 0 m. These pixels consisted of the deflation basin and the depositional lobe, so little deposition and erosion were balanced in the identified sand area. There were a few areas that changed from sand to vegetation, especially at the seaward side of the depositional lobes. These pixels showed little changes in height ranging from 0 to 0.5 m. This seemed to be the appropriate sand deposition rate whereby the seeds had the possibility to germinate and the plant growth was initiated. Although the data was not sufficient enough to determine a deposition threshold for the transition from sand to vegetation.

If such sand deposition thresholds for different transitions could be determined, it would add knowledge to the conceptual model of Schwarz et. al. (2018) shown in Figure 5. A deposition threshold for the change to sand could indicate a blowout initiation or the presence of an active dynamic blowout. While a deposition threshold for the change to vegetation could mark the transition from the geomorphological stage to the bio-geomorphological stage or even the ecological stage. This might help in predicting the blowout closure and at the same time preventing a blowout closure to keep the dynamic dune management. To achieve this, the method must be improved in determining deposition thresholds. Improvements to the method are presented in the next section 6.4.

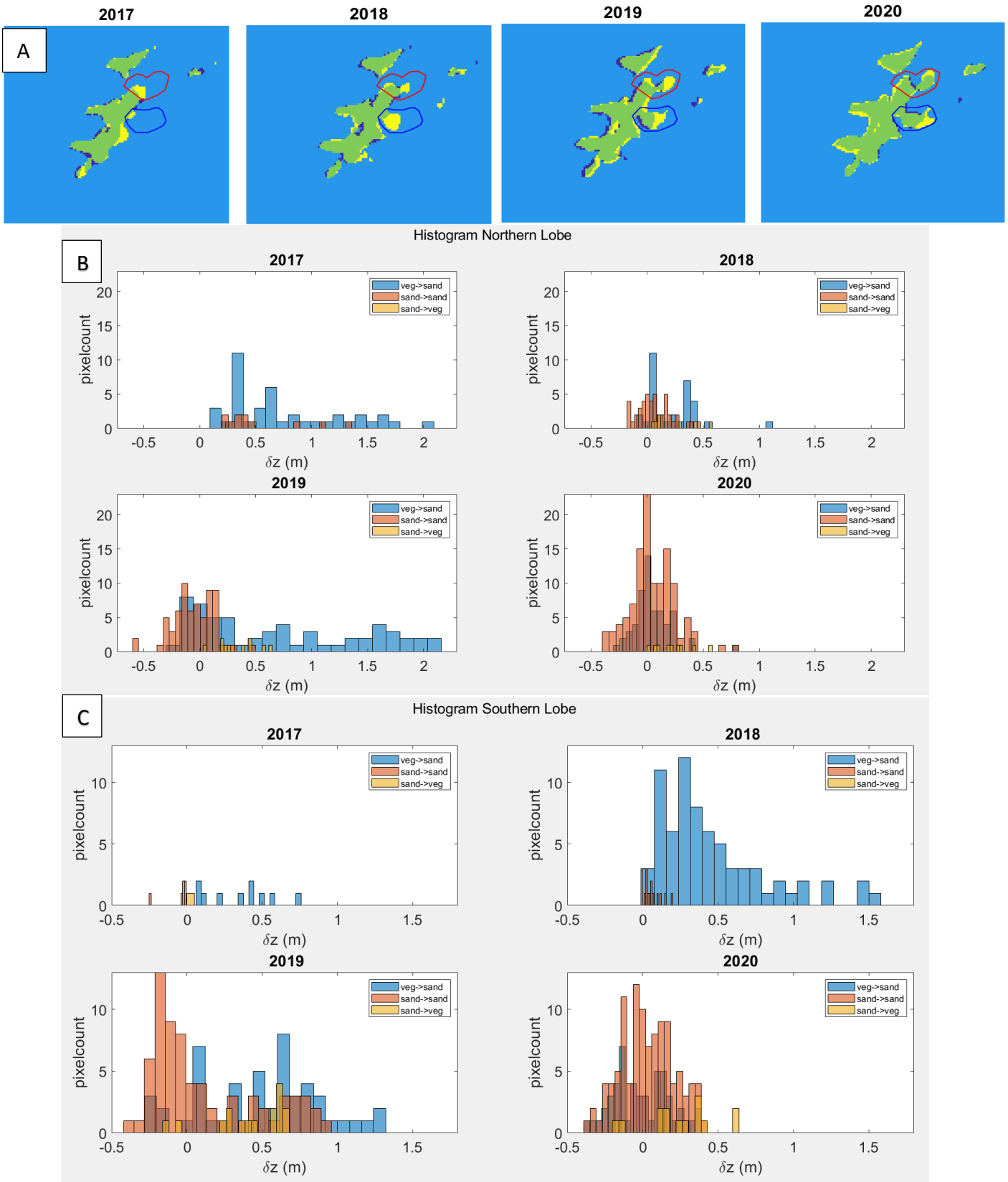

Figure 28 Noordvoort Blowout A) Classification maps from 2017 to 2020 indicating green: sand->sand, yellow: vegetation->sand, blue: sand->vegetation, with the northern and southern lobe boxes. B) Elevation change distribution of the northern depositional lobe from 2017-2020 with the classes; vegetation->sand, sand->sand and sand->vegetation. C) Elevation change distribution of the southern depositional lobe from 2017-2020 with the classes; vegetation->sand, sand->sand and sand->vegetation

6.4 Possible errors

The time series of the total data sets shown in Figures A, contain deviation of the data points. This can be a result of mixed pixels after the NDVI classification. In these pixels, both vegetation and sand appear which makes the classification harder and inconsistent. Note that all the water pixels were excluded for the NDVI classification, but it is possible that over the whole dataset some smaller temporary water areas were present increasing the mixed pixels. The number of mixed pixels is related to the 3x3m resolution of the PlanetScope satellite images. Improving the image resolution will lead to fewer mixed pixels and less deviation. This means that also smaller sudden changes on a shorter timescale can be detected which are makes the time series more reliable. Nevertheless, the pixel NVDI classification method can be used on longer timescales, year and seasonal, since sand area trends were visible.

Although the trends of the time series of all sites are missing some data. Satellite imagery was not always available or not usable due to clouds or too much shadow. Particularly this was the case in the winter months because in these months the cloud cover is larger and the dune topography in combination with the lower sun angle results in shadows. Also, the PlanetScope satellite imagery timespan was not constant. Data that is collected daily for a specific blowout, for example with a drone, would enhance the presentation of the blowout evolution. The same applies to the LiDAR airborne data which is available only once a year. Decreasing the timescale would also give better insight into possible sudden changes such as storm events. During storms, abiotic processes exceeds which can lead to large morphological changes and the initiation of blowouts (de Winter et al., 2015; Splinter et al., 2018). For example, a storm in February 2022 seemed to make about significant changes to the *Egmond-Bergen* site at first sight. A study on these storm events will give more information on the blowout development on a much shorter time scale.

7. Conclusion

This research was carried out to obtain more knowledge about the long-term (bio-)geomorphological development of six Dutch blowout complexes, *Noordvoort, Egmond-Bergen, Bloemendaal, Schouwen* and two on *Terschelling*. Based on the PlanetScope satellite imagery and the LiDAR airborne elevation data, is it shown that all six blowouts are dynamic blowout systems. The largest morphological changes occurred at the deflation basins and at the depositional lobes of the blowout complexes.

An annual positive trend in sand area from the end of 2016 to the beginning of 2021 is seen for *Schouwen* (40.9%, ~20169 m^2/year), *Egmond-Bergen* (36.2%, ~3473 m^2/year), *Noordvoort* (27.6%,~962 m^2/year), *Terschelling 2* (15.3%,~2729 m^2/year) and *Bloemendaal* (15.0%,~4486 m^2/year). *Terschelling 1* was increasing 27.5% from 2019-2021 (~8984 m^2/year). *Egmond-Bergen* and *Bloemendaal* lost sand area in 2018-2019 due to the dry summer of 2018. Relatively small areas were lost to vegetation in between the different deflation basins and/or depositional lobes. The sand area gained particularly at the edges of the blowout for *Schouwen* and *Terschelling 1* and particularly at the depositional lobes in landward direction for *Noordvoort, Egmond-Bergen, Bloemendaal* and *Terschelling 2.* They showed a distinct depositional lobe growth of 5-20 m/year. The man-made blowouts *Noordvoort* and *Bloemendaal* were both established in 2013 but differ in their connection to the beach. In this case, no connection to the beach lead to more sand area gain. While in the case of a natural blowout like *Egmond-Bergen* with a connection to the beach lead to even more sand area gain.

For every site seasonal variations in landcover were visible, especially for the bigger sites *Schouwen* and *Bloemendaal*. Peaks of the highest and lowest sand areas were determined at the beginning of the growing seasons and at the ending of the growing season. This period in which the blowout area was increasing and decreasing corresponds with the growth cycle of the vegetation. The alteration between sand and vegetation occurred all around the blowout area, especially at the edges of the depositional lobes where the thinner layer of sand is preferable for plant growth or vegetation was not covered enough by sand and grew trough the layer again. This may explains the bigger variation of *Schouwen* and *Bloemendaal* due to the larger perimeter of the blowout.

Two trends in the sand volume were seen over the years for the different sites; First an increase in cumulative sand volume due to the positive sand budget for *Egmond-Bergen (*$0.38x10^4$ m^3/year*), Bloemendaal (*$1x10^4$ m^3/year) and *Terschelling 2 (*$0.67x10^4$ m^3/year). In these blowouts more sand was deposited especially at the depositional lobes, than eroded and therefore there was a net import of sand from the beach to the blowout. Second, an increase in cumulative sand volume (due to a positive sand budget) followed by a decrease in cumulative sand volume (due to a negative sand budget) for the sites *Noordvoort (*~$1.04x10^3$ and ~$0.77x10^3$ m^3/year*), Schouwen (*~$2.2x10^4$ and ~$2.3x10^4$ m^3/year*)* and *Terschelling 1 (*~$1.75x10^4$ and ~$0.485x10^4$ m^3/year*)* was seen. The negative sand budget obtained in the same time period (2017-2021) as the sand area increases for these sites, despite the relation between volume and area. More erosion at the deflation basins, less sand input in the blowout system and a thinner layer of sand deposited landwards may explain this.

At every site the deflation basins decreased in volume while the depositional lobes increased in volume. The deepening and widening of the deflation basin happened at a relatively smaller area compared to the large deposition area at the lobes. The blowouts deepened and widened over the years with different morphological developments. For the sites *Egmond-Bergen, Schouwen* and *Terschelling 2,* which are connected to the beach, erosion at the deflation basins and deposition at the lobes happened gradually with lobe migration landwards. *Noordvoort, Bloemendaal* and *Terschelling1* showed divers profiles which induces that these findings still depend on the location of the transects and so more transects for comparison are needed to improve this section.
The erosional activity at the deflation basins was still high for the *Egmond-Bergen, Bloemendaal* and *Schouwen* while *Noordvoort* and *Terschelling 2* seemed to reach the maximum erosional level of their deflation basins. However the morphological changes and therefore the abiotic processes of aeolian sand transport would suggest that all blowout sites were still in the geomorphological stage following the conceptual model of Schwarz et. al. (2018). Histograms with the distribution of the heights change for the different landcover changes may determine a deposition threshold for a stage transition. Nevertheless, the elevation and satellite imagery data were not sufficient enough to determine specific deposition thresholds in this study.

So overall, no strong relation in size, age, man-made/natural or the beach connection which may drive the sand area or sand volume increment difference, was found by looking at these results. The characteristics of the blowouts differ too much to find a clear answer on which factors determine the difference in developments. Further research in sand budgets and sand deposition thresholds on more blowouts with an improved satellite resolution and time span should be done. This will contribute to the understanding of the blowout development and the prediction of blowout closure to keep the dynamic dune management.

References

Arens, B. (2014). Verstuivingsonderzoek Kop van Schouwen . *Bureau Strand- En Duinonderzoek* .

Arens, S. M., Loffler, M. A. M., & Nuijen, E. M. (2007). Evaluatie dynamisch kustbeheer Friese Waddeneilanden. *Bureau Voor Stranden Duinonderzoek*.

Arens, S. M., Mulder, J. P. M., Slings, Q. L., Geelen, L. H. W. T., & Damsma, P. (2013). Dynamic dune management, integrating objectives of nature development and coastal safety: Examples from the Netherlands. *Geomorphology*, *199*, 205–213. https://doi.org/10.1016/j.geomorph.2012.10.034

Arens, S., Slings, Q., & de Vries, C. (2004). Mobility of a remobilised parabolic dune in Kennemerland, The Netherlands. *Elsevier*. https://doi.org/10.1016/j.geomorph.2003.09.014

Balke, T., Herman, P. M. J., & Bouma, T. J. (2014). Critical transitions in disturbance-driven ecosystems: Identifying windows of opportunity for recovery. *Journal of Ecology*, *102*(3), 700–708. https://doi.org/10.1111/1365-2745.12241

Barchyn, T. E., & Hugenholtz, C. H. (2012). Aeolian dune field geomorphology modulates the stabilization rate imposed by climate. *Journal of Geophysical Research: Earth Surface*, *117*(F2), 2035. https://doi.org/10.1029/2011JF002274

Barchyn, T. E., & Hugenholtz, C. H. (2013a). Reactivation of supply-limited dune fields from blowouts: A conceptual framework for state characterization. *Geomorphology*, *201*, 172–182. https://doi.org/10.1016/J.GEOMORPH.2013.06.019

Barchyn, T. E., & Hugenholtz, C. H. (2013b). Reactivation of supply-limited dune fields from blowouts: A conceptual framework for state characterization. *Geomorphology*, *201*, 172–182. https://doi.org/10.1016/J.GEOMORPH.2013.06.019

Bate, G., & Ferguson, M. (1996). Blowouts in coastal foredunes. *Landscape and Urban Planning*, *34*(3–4), 215–224. https://doi.org/10.1016/0169-2046(95)00218-9

Bochev-Van der Burgh L. M., Wijnberg, K. M., & Hulscher, S. J. (2011). Decadal-scale morphologic variability of managed coastal dunes. *Coastal Engineering, 58(9), 927-936.*

Cheplick, G. P., & Grandstaff, K. (1997). Effects of sand burial on purple sandgrass (Triplasis purpurea): the significance of seed heteromorphism. *Plant Ecology 1997 133:1*, *133*(1), 79–89. https://doi.org/10.1023/A:1009733128430

Cooper, W. S. (1958). Coastal sand dunes of Oregon and Washington. *Geological Society of America - Memoir 72*, 169.

Corenblit, D., Baas, A., Balke, T., Bouma, T., Fromard, F., Garófano-Gómez, V., González, E., Gurnell, A. M., Hortobágyi, B., Julien, F., Kim, D., Lambs, L., Stallins, J. A., Steiger, J., Tabacchi, E., & Walcker, R. (2015). Engineer pioneer plants respond to and affect geomorphic constraints similarly along water–terrestrial interfaces world-wide. *Global Ecology and Biogeography*, *24*(12), 1363–1376. https://doi.org/10.1111/GEB.12373

Davidson-Arnott, R. G. D., & Law, M. N. (1996). Measurement and prediction of long-term sediment supply to Coastal Foredunes. *Journal of Coastal Research 12*, 654-663.

Davies, J. L. (1980). Geographical Variation in Coastal Development. *Longman, London*, 204.

de Winter, R. C., Gongriep, F., & Ruessink, B. G. (2015). Observations and modeling of alongshore variability in dune erosion at Egmond aan Zee, the Netherlands. *Coast. Eng. 2015, 99, 167–175.*

Everard, M., Jones, L., and, B. W.-A. conservation marine, & 2010, undefined. (2010). Have we neglected the societal importance of sand dunes? An ecosystem services perspective. *Agris.Fao.Org*. https://doi.org/10.1002/aqc.1114

Feagin, R. A., Figlus, J., Zinnert, J. C., Sigren, J., Martínez, M. L., Silva, R., Smith, W. K., Cox, D., Young, D. R., & Carter, G. (2015). Going with the flow or against the grain? The promise of vegetation

for protecting beaches, dunes, and barrier islands from erosion. *Frontiers in Ecology and the Environment*, *13*(4), 203–210. https://doi.org/10.1890/140218

Frazier, A., & Hemingway, B. (2021). A Technical Review of Planet Smallsat Data: Practical Considerations for Processing and Using PlanetScope Imagery. *Remote Sensing 2021, Vol. 13, Page 3930*, *13*(19), 3930. https://doi.org/10.3390/RS13193930

Garès, P. A., & Pease, P. (2015). Influence of topography on wind speed over a coastal dune and blowout system at Jockey's Ridge, NC, USA. *Earth Surface Processes and Landforms*, *40*(7), 853–863. https://doi.org/10.1002/ESP.3670

Gares, P., & Nordstrom, K. (1987). *DYNAMICS OF A COASTAL FOREDUNE BLOWOUT AT ISLAND BEACH STATE PARK, NJ.* https://www.researchwithrutgers.com/en/publications/dynamics-of-a-coastal-foredune-blowout-at-island-beach-state-park

Ghaderpour, E. (2021). JUST: MATLAB and python software for change detection and time series analysis. *GPS Solutions 2021 25:3*, *25*(3), 1–7. https://doi.org/10.1007/S10291-021-01118-X

Hesp, P. (2002). Foredunes and blowouts: initiation, geomorphology and dynamics. *Geomorphology*, *48*(1–3), 245–268. https://doi.org/10.1016/S0169-555X(02)00184-8

Hesp, P. A. (1989). A review of biological and geomorphological processes involved in the initiation and development of incipient foredunes. *Proceedings of the Royal Society of Edinburgh, Section B: Biological Science*, *96*, 181–201. https://www.cambridge.org/core/journals/proceedings-of-the-royal-society-of-edinburgh-section-b-biological-sciences/article/review-of-biological-and-geomorphological-processes-involved-in-the-initiation-and-development-of-incipient-foredunes/56D70F84F9D032DEFB9CAB73EDE08225

Hesp, P. A., & Hyde, R. (1996). Flow dynamics and geomorphology of a trough blowout. *Sedimentology*, *43*(3), 505–525. https://doi.org/10.1046/J.1365-3091.1996.D01-22.X

Hesp, P. A., & Walker, I. J. (2012). Three-dimensional æolian dynamics within a bowl blowout during offshore winds: Greenwich Dunes, Prince Edward Island, Canada. *Aeolian Research*, *3*(4), 389–399. https://doi.org/10.1016/J.AEOLIA.2011.09.002

Hugenholtz, C. H., & Wolfe, S. A. (2006). Morphodynamics and climate controls of two aeolian blowouts on the northern Great Plains, Canada. *Earth Surface Processes and Landforms*, *31*(12), 1540–1557. https://doi.org/10.1002/ESP.1367

Huggett, R. J. (2007). Fundamentals of Geomorphology. In *Fundamentals of Geomorphology*. https://doi.org/10.4324/9781315674179

Lee, P. C. (1995). The effect of gap dynamics on the size and spatial structure of Solidago sempervirens on primary coastal dunes. *Journal of Vegetation Science*, *6*(6), 837–846. https://doi.org/10.2307/3236397

Maun, M. (2009). The biology of coastal sand dunes. In *Oxford University Press: Oxford, UK.* Oxford University Press. https://books.google.com/books?hl=nl&lr=&id=Z9XPa7-Je8YC&oi=fnd&pg=PR11&dq=The+Biology+of+Coastal+Sand+Dunes&ots=9NDgWDhs0v&sig=N-BG1WBnNlxie8rCRekColVhTIM

Maun, M. A. (1994). Adaptations enhancing survival and establishment of seedlings on coastal dune systems. *Vegetatio 1994 111:1*, *111*(1), 59–70. https://doi.org/10.1007/BF00045577

Maun, M. A. (1998). Adaptations of plants to burial in coastal sand dunes. *J. Bot. 1998, 76, 713–738.* https://doi.org/10.1139/B98-058

Miyanishi, K., & Johnson, E. A. (2007). Coastal dune succession and the reality of dune processes. *Plant Disturb. Ecol. Process Response 2007, 249–282.* https://doi.org/10.1016/B978-0-12-818813-2.00007-1

Musick, H. B., Trujillo, S. M., & Truman, C. R. (1996). Wind-tunnel modelling of the influence of vegetation structure on saltation threshold. *Earth Surface Processes and Landforms* , *21*, 589–

606. https://onlinelibrary.wiley.com/doi/abs/10.1002/(SICI)1096-9837(199607)21:7%3C589::AID-ESP659%3E3.0.CO;2-1

Nickling, W., Dunes, R. D.-A. C. S., & 1990, undefined. (1990). Beaches and coastal sand dunes. *Researchgate.Net*. https://www.researchgate.net/profile/Robin-Davidson-Arnott/publication/274192369_Aeolian_Sediment_Transport_on_Beaches_and_Coastal_Sand_dunes/links/5517ee210cf29ab36bc2f1f3/Aeolian-Sediment-Transport-on-Beaches-and-Coastal-Sand-dunes.pdf

Planet Labs Inc. (2021). *PLANET IMAGERY PRODUCT SPECIFICATIONS*. https://assets.planet.com/docs/Planet_Combined_Imagery_Product_Specs_letter_screen.pdf

Pluis, J. L. A., & van Boxel, J. H. (1993). Wind velocity and algal crusts in dune blowouts. *Catena 1993, 20, 581–594.* https://doi.org/10.1016/0341-8162(93)90018-K

Pye, K., Blott, S. J., & Howe, M. A. (2014). Coastal dune stabilization in Wales and requirements for rejuvenation. *Journal of Coastal Conservation*, *18*(1), 27–54. https://doi.org/10.1007/S11852-013-0294-8

Pye, K., & Tsoar, H. (1990). *Aeolian Sand and Sand Dunes* (Unwin Hyman).

Ruessink, B. G., Arens, S. M., Kuipers, M., & Donker, J. J. A. (2018). Coastal dune dynamics in response to excavated foredune notches. *Aeolian Research*, *31*, 3–17. https://doi.org/10.1016/j.aeolia.2017.07.002

Schwarz, C., Brinkkemper, J., & Ruessink, G. (2018). Feedbacks between Biotic and Abiotic Processes Governing the Development of Foredune Blowouts: A Review. *Journal of Marine Science and Engineering 2019, Vol. 7, Page 2*. https://doi.org/10.3390/JMSE7010002

Sherman, D. J., & Lyons, W. (1994). Beach-state controls on aeolian sand delivery to coastal dunes. *Physical Geography*, *15*(4), 381–395. https://doi.org/10.1080/02723646.1994.10642524

Smyth, T. A. G., Jackson, D. W. T., & Cooper, J. A. G. (2012). High resolution measured and modelled three-dimensional airflow over a coastal bowl blowout. *Geomorphology*, *177–178*, 62–73. https://doi.org/10.1016/J.GEOMORPH.2012.07.014

Splinter, K. D., Kearney, E. T., & Turner, I. L. (2018). Drivers of alongshore variable dune erosion during a storm event: Observations and modelling. *Coastal Engineering*, *131*, 31–41. https://doi.org/10.1016/J.COASTALENG.2017.10.011

Wilson, J. D., Finnigan, J. J., & Raupach, M. R. (1998). A first-order closure for diturbed plant-canopy flows, and its application to winds in a canopy on a ridge. *Quarterly Journal of the Royal Meteorological Society*, *124*(547), 705–732. https://doi.org/10.1002/QJ.49712454704

Zarnetske, P. L., Ruggiero, P., Seabloom, E. W., & Hacker, S. D. (2015). Coastal foredune evolution: the relative influence of vegetation and sand supply in the US Pacific Northwest. *Journal of The Royal Society Interface*, *12*(106). https://doi.org/10.1098/RSIF.2015.0017